



Groundwater Salinity and Particulate Organic Carbon Flux Control Benthic Habitats in Anchialine Environments on Millennial Timescales

Jacque N. Cresswell¹ and Peter J. van Hengstum^{2,3*}

¹ Department of Science and Business, Galveston College, Galveston, TX, United States, ² Department of Oceanography, Texas A&M University, College Station, TX, United States, ³ Department of Marine and Environmental Science, Texas A&M University at Galveston, Galveston, TX, United States

OPEN ACCESS

Edited by:

Luis M. Mejía-Ortiz,
University of Quintana Roo, Mexico

Reviewed by:

Nuria Torrescano,
The South Border College (ECOSUR),
Mexico

Neven Cukrov,
Ruder Bošković Institute,
Croatia

*Correspondence:

Peter J. van Hengstum
vanhenp@tamug.edu

Specialty section:

This article was submitted to
Marine Ecosystem Ecology,
a section of the journal
Frontiers in Marine Science

Received: 10 March 2022

Accepted: 31 March 2022

Published: 06 May 2022

Citation:

Cresswell JN and van Hengstum PJ
(2022) Groundwater Salinity
and Particulate Organic Carbon
Flux Control Benthic Habitats
in Anchialine Environments
on Millennial Timescales.
Front. Mar. Sci. 9:893867.
doi: 10.3389/fmars.2022.893867

The environmental conditions and habitats in Bermudian underwater caves have responded to vertical aquifer migration and groundwater salinity changes associated with sea-level rise since the last glacial maximum. Recently, a large database of modern benthic foraminifera in Bermudian caves were found to be highly sensitive to both the amount and source of particle organic carbon (POC) transported to the sediment-water interface, consistent with similar timewise analysis of foraminifera in a Mexican flooded cave. Here we provide evidence that while benthic meiofaunal communities in Bermuda's underwater caves are primarily controlled by groundwater salinity changes on millennial timescales from sea-level change, they are secondarily controlled by the POC source and supply deposited in the cave through time. Benthic foraminiferal assemblages were evaluated in the best-preserved stratigraphic succession currently known from an underwater cave. In the case of Palm Cave, POC flux changes were driven by changes in seawater-groundwater circulation dynamics caused by flooding on the carbonate banktop, and the inherited geometry of the cave system itself. These results demonstrate that benthic meiofaunal communities in anchialine environments are highly sensitive to changes in the source and quantity of POC through time. This work also enables a better understanding of the environmental conditions associated with preserved meiofaunal remains in global cave sediment. These results indicate that if the POC flux to the subsurface increases from coastal urbanization on karst landscapes, subsurface anchialine communities are likely to respond.

Keywords: sea level, anchialine, subterranean estuaries, karst, foraminifera, Bermuda

1 INTRODUCTION

Karst subterranean estuaries (KSEs) are created from the two- and three-way mixing of saline groundwater, rain, and oceanic water in the subsurface on carbonate landscapes, which creates an anchialine habitat continuum in the subsurface (van Hengstum et al., 2019). Subterranean estuaries can occur on carbonate, volcanic, or siliciclastic coastlines (Moore, 1999; Gonneea et al., 2014), but

carbonate landscapes are often perforated by cave networks that allow for direct human exploration and scientific observation within the subterranean estuary. Traditionally, the adjective ‘anchialine’ had been used to describe the unique fauna and ecosystems that live in volcanic and karst subterranean estuaries (Stock et al., 1986; Bishop et al., 2015). Over the last 2 million years, anchialine environments have endured repeated vertical migration in global carbonate platforms in response to orbitally-forced ice sheet dynamics and sea-level change (Shinn et al., 1996; van Hengstum et al., 2011; Gregory et al., 2017), which creates the aquatic and salinity boundary conditions for subsurface environmental change at given geographic locales and perhaps contributes to subsurface evolution (Riedl and Ozretić, 1969; Sanz and Platvoet, 1995; van Hengstum et al., 2019). On much shorter timescales (10^2 and 10^3 years), however, the factors controlling and impacting both benthic and pelagic communities in anchialine environments is less clear, and yet this knowledge is required to fully understand how anchialine environments and communities will change from marine climate change and coastal urbanization in the 21st century.

Similar to coastal estuaries, KSE can be divided into lower estuarine zone of saline groundwater that is intruding from the adjacent ocean, and an upper estuarine zone of meteoric water that is resupplied by infiltrating rain. Modern transect studies have investigated the regulators of environmental conditions and biologic response in meteoric lenses, across modern zones of mixing or density interfaces, and in the saline groundwater (Fichez, 1991a; Fichez, 1991b; van Hengstum et al., 2008; van Hengstum and Scott, 2011; Radolović et al., 2015; Brankovits et al., 2017; Chávez-Solís et al., 2020; Brankovits et al., 2021; Ballou et al., 2022). Like their subaerial counterparts, however, the geochemical and biological processes that occur within each individual water mass are complex, and necessarily impact their hosted benthic and pelagic fauna.

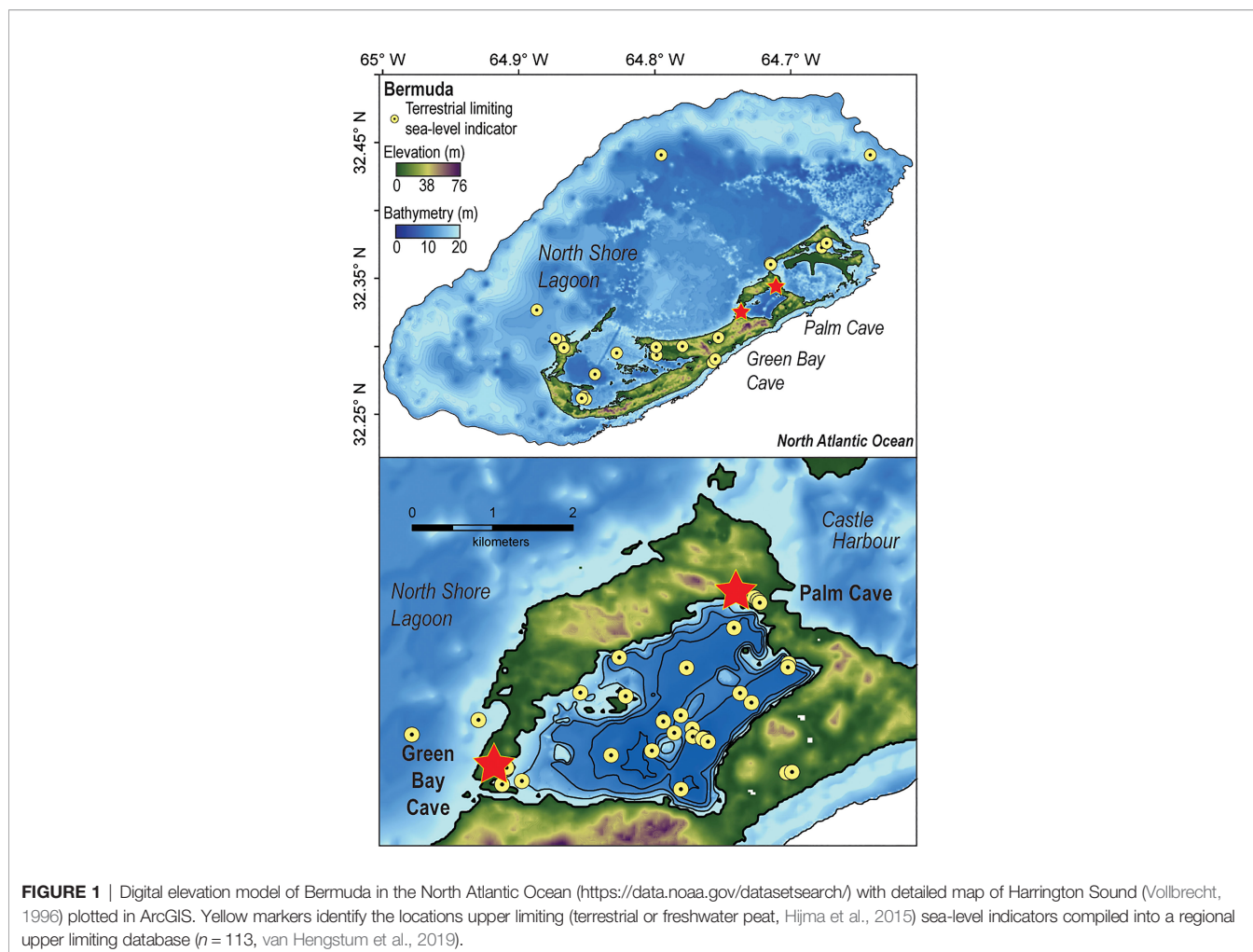
Here we use subfossil benthic foraminifera preserved in sediment cores from Palm Cave in Bermuda to investigate secondary factors that control benthic anchialine habitat development on millennial timescales. Palm Cave has the best-preserved stratigraphic record yet known from an underwater cave, and it spans the last ~10,000 years. There is clear stratigraphic evidence documenting how the cave was first flooded by a meteoric lens from sea-level rise ~9500 years ago, followed by multiple environmental changes driven by Holocene regional oceanographic and groundwater development. Benthic foraminifera are unicellular protists that are highly sensitive to environmental gradients (Jorissen et al., 1995; Scott et al., 2001; Murray, 2006), and they have a great preservation potential in the sediment of aquatic caves and groundwater-fed habitats on carbonate landscapes (van Hengstum et al., 2009; van Hengstum and Scott, 2011; Bergamin et al., 2018; Romano et al., 2018; Bergamin et al., 2020; Romano et al., 2020; Cresswell and van Hengstum, 2021). The new data presented here documents that benthic anchialine habitats are first established by the groundwater mass (primary factor), which is under sea-level forcing, followed by particulate organic carbon (POC) source and quantity fluxed into the karst subterranean estuary through time (secondary factor).

2 STUDY SITE AND PREVIOUS WORK

The North Atlantic archipelago of Bermuda is a ~35 million year old volcanic seamount capped by carbonates that have weathered into a mature karst landscape (Bretz, 1960; Land et al., 1967; Vacher and Rowe, 1997; Hearty, 2002). Large cave chambers in Bermuda dissolved during both phreatic and vadose conditions during the Quaternary, and they are now connected by fissures from extensive collapse events (Palmer et al., 1977; Mylroie et al., 1995). Drilling evidence indicates that the carbonate cap on Bermuda extends up to 80 m below modern sea level (Pirsson, 1914; Pirsson and Vaughn, 1917; Sayes, 1931; Woolard and Ewing, 1939), so all carbonates were in the unsaturated (vadose) zone during the last glacial maximum when relative sea level was at least 120 meters below modern sea level (Lisiecki and Raymo, 2005; Rohling et al., 2014). Fossil foraminifera preserved in the Pirsson well were investigated by Joseph Cushman (Sayes, 1931) and Carmen (1927). While fossilized foraminiferal remains were in poor condition and not chronologically diagnostic, Cushman thought the foraminifera were likely Miocene-aged or younger (as described in Sayes, 1931).

Palm Cave is located on the isthmus between Harrington Sound and Castle Harbour (**Figure 1**), which hosts the greatest density of caverns on the island. Harrington Sound has been extensively studied, including its flooding and environmental change in response to deglacial sea-level rise (Vollbrecht, 1996) and modern marine habitats and seawater circulation (Neumann, 1965; Morris et al., 1977; Bates, 2017). Palm Cave is accessed through at least seven entrances that are interconnected by underwater conduits in the modern phreatic zone (one entrance at 32.34°, -64.71°). These entrances provide physical openings that allow terrestrial nutrients and sediments from the surrounding forest landscape to enter the subsurface aquatic environments below. Vertically, the cave extends to a maximum depth of 23 m below modern sea level (mbsl), and the cave does not expose a volcanic-limestone lithologic contact. Currently, tidally-forced seawater and nutrient exchange occurs between Harrington Sound and Palm Cave through a narrow inlet or entrance called ‘Cripplegate’: a shallow (<0.6 mbsl) and narrow (<0.6 m high) passage that is not humanly passable (see transect C in **Figure 2**). Currently, Palm Cave is entirely flooded by oxygenated saline groundwater (>3 mg/L) that tidally circulates with seawater from the adjacent coastal lagoons (Cate, 2009; Stoffer, 2013). The narrow width of the host isthmus combined with high porosity of the local carbonate means that only a transient or shallow (<50 cm) meteoric lens (freshwater, brackish) is formed in the area of the Palm Cave (Little and van Hengstum, 2019), and the cave does not discharge meaningful amounts of fresh groundwater.

Sediment coring in 2015 produced 14 push cores that were extensively radiocarbon dated ($n = 51$; See **Supplementary Information Table S1**) to reconstruct environmental change in Palm Cave since the last glacial maximum (van Hengstum et al., 2019). Indeed, each individual collected core has hiatuses in deposition (i.e., disconformities), but collectively, they provide a complete picture of groundwater and habitat changes in this area of the karst subterranean estuary during the Holocene. The cave



stratigraphy can be grossly divided into four sedimentary facies (See **Supplementary Information Tables S2, S3**), which can be further subdivided into seven units (**Figure 3**). The oldest deposits are pre-Holocene (>11,600 years ago) terra rosa paleosols, that contain coarse-grained sediments with a deep red color, and no fossil material. Mineralogically, they are similar to Bermudian Pleistocene-aged terra rosa paleosols, and include crandallite, kaolinite, quartz, and goethite (Muhs et al., 2012) (See van Hengstum et al., 2019). Sapropel accumulated from ~9750 to ~8370 Cal yrs BP, which could be divided into separate layers by color, and they contained both freshwater and brackish ostracodes and foraminifera. The organic-rich deposits provide evidence for the freshwater and brackish aquatic habitats in the Palm Cave from 9750 ± 210 to 8370 ± 30 Cal yrs BP when a fresh to oligohaline meteoric lens first flooded the cave. Next, iron-rich carbonate deposits formed in the deepest areas of the Palm Cave (base of core 3, 15, and 9, and intercalated within cores 4,10,11 and 9). Mixing of the anoxic saline groundwater and oxygenated water mass likely created an 'iron curtain' at the sediment-water interface with a distinctive orange-hued, and fine textured deposit that contained POC primarily from a marine source.

By 6600 ± 70 Cal yrs BP, carbonate sediment began deposition throughout Palm Cave.

3 METHODS

The most expanded sedimentary archives from Palm Cave were selected for a detailed analysis of benthic environmental change (cores 2, 4, 7, 10, 14, and 15, **Figure 3**). Benthic foraminifera were first concentrated by wet sieving 0.63 cm^3 to 1.25 cm^3 of bulk sediment sub-samples over standard $63 \mu\text{m}$ screen meshes, and the remaining coarse sediment residues were split into equal aliquots using a wet splitter (Scott and Hermelin, 1993) to enable representative census counts of ~300 individuals per sample. Little and van Hengstum (2019) determined that a $63 \mu\text{m}$ screen provides an adequate representation of the taxa present in underwater caves. Individual benthic foraminifera were wet picked onto micropaleontological slides and identified to generic level, with taxonomy confirmed by scanning electron microscopy of representative individuals (**Figure 4**) and literature comparisons (Carmen, 1927; Bermúdez, 1949; Loeblich and Tappan, 1987;

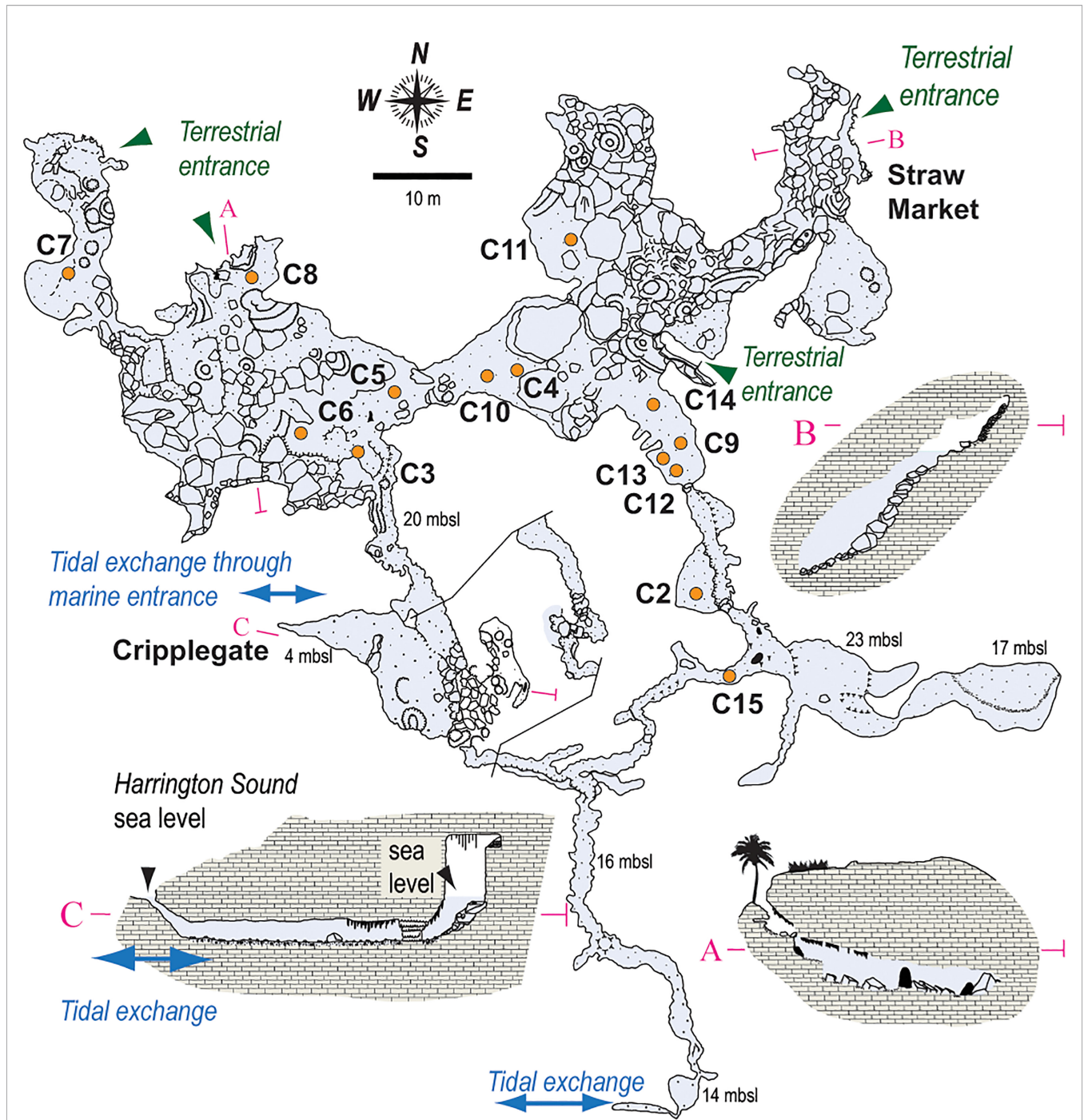
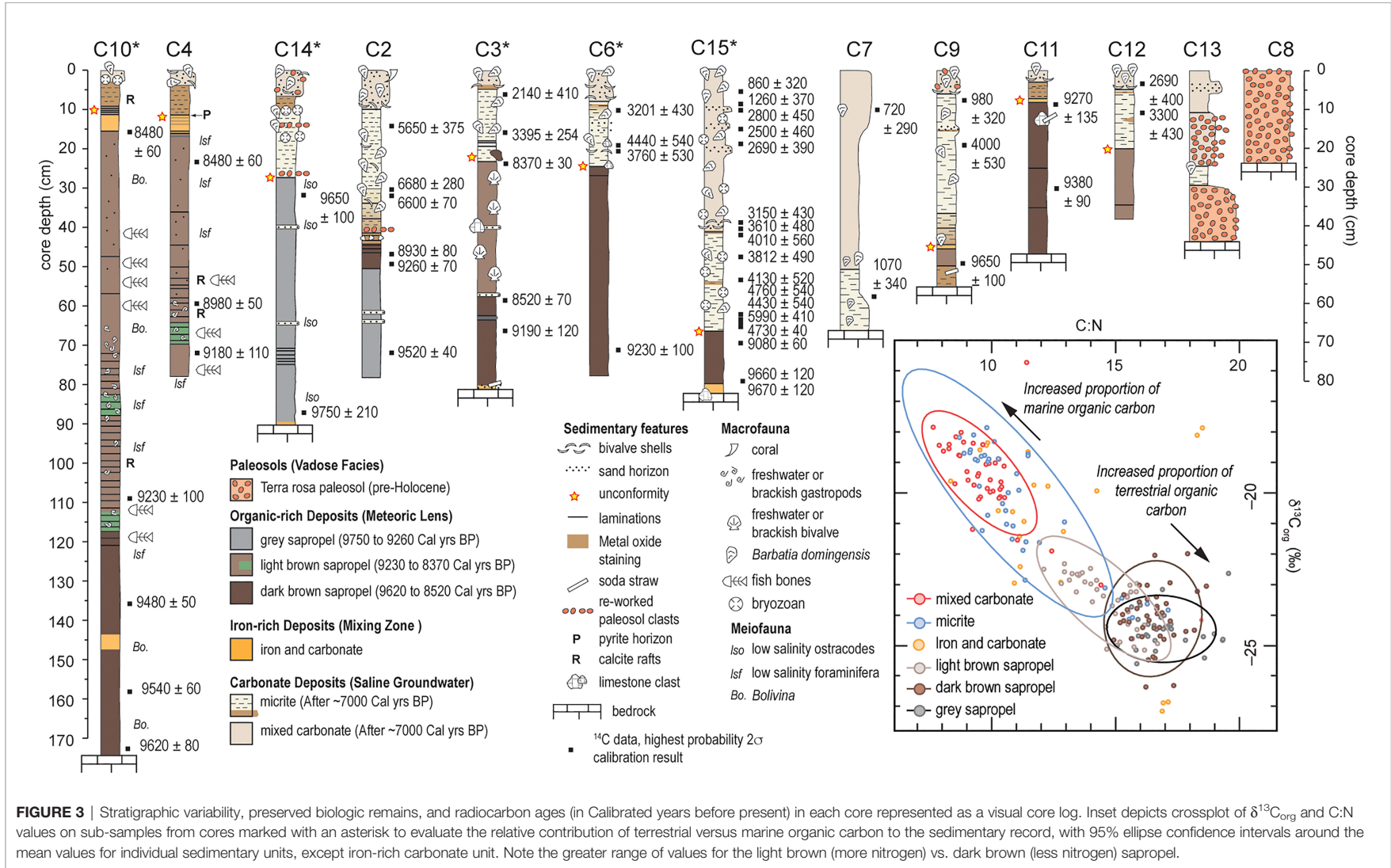


FIGURE 2 | Survey of the Palm Cave System, with core locations (orange circles) noted throughout. The narrow opening at Cripplegate (<1 m water depth) is the only known direct connection to open water. Tidal currents most elevated along eastern passages, which suggests there is perhaps also volumetrically-significant tidal-exchange of seawater between Harrington Sound and Palm Cave through the southern passages. After original cave survey drawn by Jason Richards.

Javaux and Scott, 2003; van Hengstum and Scott, 2011; Little and van Hengstum, 2019). An original data matrix containing 110 samples and 64 taxonomic observations was produced from the Palm Cave sediment cores, with a total 38,618 individual foraminifera tests counted as part of this study. However, taxa

were considered insignificant and removed from further multivariate cluster analysis if the proportional abundance was less than the calculated standard error at a 95% confidence interval in all samples (Patterson and Fishbein, 1989), or if the species was present in only one sample. A final data matrix contained 110



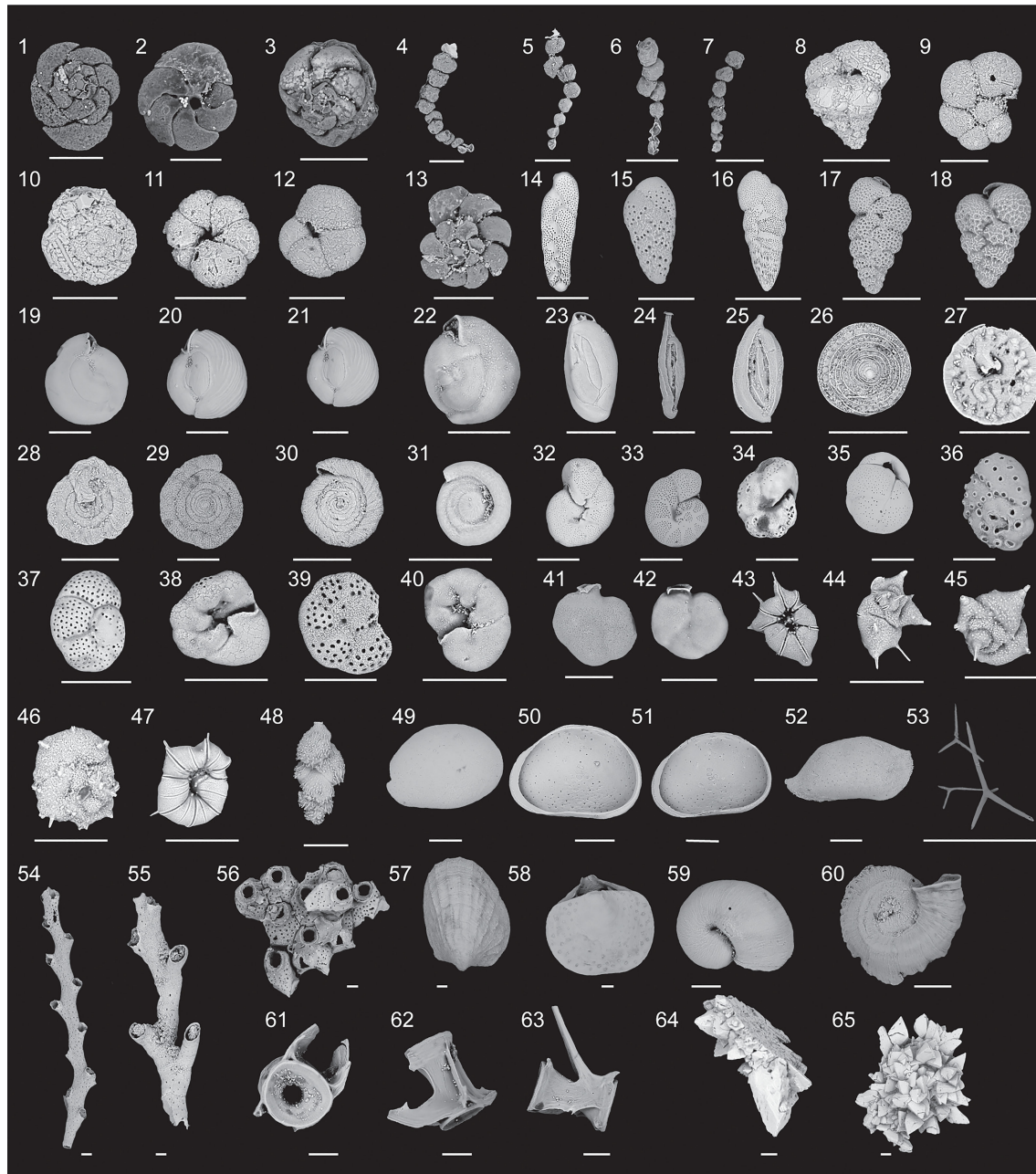


FIGURE 4 | Scanning electron micrographs of representative biological and sedimentary remains (1-48, benthic foraminifera; 49- 65, other). 1-3, Dorsal and ventral views of *Tiphrotricha comprimata* (Cushman and Brönnimann, 1948). 4-7, *Polysaccammina ipohalina* (Scott, 1976). 8, *Eggerella scabra* (Williamson, 1858). 9, *Labrospira evoluta* (Nattland, 1938). 10-12, Dorsal and ventral views of *Trochammina quadriloba* (Höglund, 1947). 13, *Entzia macrescens* (Brady and Robertson, 1870). 14, *Bolivina pseudopunctata* (Höglund, 1947). 15, *Bolivina paula* (Cushman and Ponton, 1932). 16, *Bolivina striatula* (Cushman, 1922). 17-18, *Bolivina variabilis* (Williamson, 1858). 19-22, *Miliolinella circularis* (Bornemann, 1855). 23, *Quinqueloculina bosciana* (D'Orbigny, 1839). 24, *Spirophthalmidium emaciatum* (Haynes, 1973). 25 *Sigmollina tenuis* (Czjzek, 1848). 26-27, *Patellina corrugata* Williamson (1858). 28, *Mychostomina revertens* (Rhumbler, 1906). 29- 30, *Spirillina vivipara* (Ehrenberg, 1843). 31, *Cyclogyra involvens* (Reuss, 1850). 32-33, *Melonis barleeianum* (Williamson, 1858). 34, *Nonion pauperatum* (Balkwill and Wright, 1885). 35, *Globocassidulina subglobosa* (Brady, 1881). 36, Dorsal view of *Svratkina australiensis* (Chapman et al., 1934). 37- 40, Dorsal and ventral views of *Rosalina* spp. 41-43, *Siphonina temblorensis* (Garrison, 1959). 43-45, Dorsal and ventral views of *Rotaliella arctica* (Scott and Vilks, 1991). 46-47, Dorsal and ventral views of *Heronallenita* spp. 48, *Trifarina occidentalis* (Cushman, 1922). 49 dorsal view of ostracode *Cypridopsis vidua* (Müller). 50-51, ventral view of ostracode *Cypridopsis vidua* (Müller), 52, dorsal view of *Paranesidea sterreri* Maddocks (Maddocks and Illife, 1986). 53, Sponge spicules. 54- 55, Branching bryozoans. 56, Cheilostome bryozoan. 57, Bivalve. 58, Brachiopod. 59, Mollusk. 60, Encrusting tube-worm. 61- 63, Teleost (Fish) vertebrae. 64-65, Calcite rafts. All scale bars represent 100 μ m.

samples with 49 taxonomic observations after insignificant taxa were removed (See **Supplementary Database**). The final data of raw count abundances was then converted to proportional abundances in the 'vegan' package in RStudio (Oksanen et al., 2013).

Unconstrained Q-mode cluster analysis was used to emphasize community-level patterns (Legandre and Legendre, 1998) and identify assemblages that are ecologically meaningful. Prior to cluster analysis, the proportional abundances were square root transformed to minimize the impact of dominant species and to better compare community structure (Legendre and Legendre, 1998). Samples were then clustered using an unweighted paired group averaging algorithm and the Bray-Curtis dissimilarity index ['simprof' function in 'clustsig' package, and 'vegdist' function in 'vegan' package] (Clarke et al., 2008; Oksanen et al., 2013; Whitaker and Christman, 2014). Lastly, a stratigraphic plot was created in RStudio to compare membership of dominant benthic foraminifera in relation to the previously generated assemblages identified in the dendrogram from cluster analysis. The final stratigraphic plot only shows taxa with 5% proportional abundance in at least 1 sample, with the raw graphic design generated using the 'stratplot' function in the 'rioja' package (Juggins, 2015).

Finally, detailed benthic foraminiferal results are compared to the previously measured bulk textural (coarse particle content and bulk organic matter) and geochemical properties of their samples (stable carbon isotopic value: $\delta^{13}\text{C}_{\text{org}}$ and the C:N ratio of bulk sedimentary organic matter). Detailed methods regarding their measurement are documented elsewhere (van Hengstum et al., 2019). In short, the relative proportion of terrestrial versus marine organic matter accumulating at each core level was estimated by a simple 2-endmember isotopic mass balance: $\delta X_i = F_m \cdot \delta X_m + F_t \cdot \delta X_t$; where $1 = F_t + F_m$ (van Hengstum et al., 2011). Since the carbon isotopic ratio of bulk terrestrial organic matter is similar to the remains of organic matter produced by primary productivity in freshwater settings (-26 to -28‰) (France, 1995; Lamb et al., 2006), differentiating these sources can only be achieved with additional organic biomarkers or indices. The 2-endmember model also cannot differentiate whether marine organic matter is either from pelagic sources (i.e., seston), or is derived from the remains of more carbon-isotopically enriched seagrass beds that are currently abundant in Bermudian coastal lagoons (Fourqurean et al., 2015; Fourqurean et al., 2019). However, a simple binary conceptual model of organic matter sourcing is useful for providing a first-order understanding on the source of organic matter being deposited in an underwater cave on millennial timescales. The terrestrial endmember (δX_t) was -27.7‰ as measured on a sample from Deep Blue Cave in Bermuda (Little and van Hengstum, 2019), and the marine endmember (δX_m) was -15.2‰ as measured on a sample from Palm Cave (Cresswell & van Hengstum, 2021).

4 FORAMINIFERAL RESULTS

Abundant benthic foraminifera are preserved in the stratigraphy of Palm Cave. Two broad groupings of samples can be differentiated at a Bray-Curtis dissimilarity index of ~ 0.8 that are assemblages of foraminifera that most likely lived in a

meteoric lens (fresh to brackish water, upper estuary) versus saline groundwater (marine, lower estuary). However, dividing the dendrogram at Bray-Curtis dissimilarity index of 0.5 provides a more nuanced grouping of the samples into 7 assemblages that are so-named in relation to salinity, POC quantity and source, and likely tidal relationship (**Figure 5**).

4.1 Subtidal Assemblage (9540 \pm 60 to 9480 \pm 50 Cal yrs BP)

The oldest sediment preserved in the deepest cave areas is a dark brown sapropel and it contains the subtidal assemblage. This assemblage is located in core 4 (15 cm), core 10 (140 to 160 cm) and core 15 (67 cm), and it is characterized by organic carbon that is primarily from the terrestrial surface ($\delta^{13}\text{C}_{\text{org}}$ mean: -23.1‰ ; terrestrial organic carbon mean: 62.8%), abundant total organic carbon content (mean: 19.3%), and a texture of very fine silt (mean: 4.3 μm). The subtidal assemblage is diverse ($H' = 2.3$; $R = 26$) and dominated by *Bolivina* spp. (mean: 36.4%), and epifaunal rotaliids such as *Rosalina* spp. (mean: 15.1%), *Globocassidulina subglobosa* (mean 10.8%), and *Syratkinia australiensis* (mean: 3.5%; **Table 1**). Radiocarbon ages in the dark brown sapropel at 67 cm in core 15, at 140 cm and 160 cm, and core 10 were 9080 \pm 60, 9480 \pm 50, and 9540 \pm 60 Cal yrs BP, respectively.

4.2 Low Oligohaline Assemblage (9180 Years Ago)

The low oligohaline assemblage ($n = 4$ samples) is located at the base of the light brown sapropel sediments in core 4 (72 to 78 cm) and in core 10 (120 cm). The silty organic-rich sediment (medium silt mean: 27.7 μm) is primarily terrestrial in origin (terrestrially-derived organic carbon mean: 72.2%), based on the stable carbon isotopic content of the bulk organic matter ($\delta^{13}\text{C}_{\text{org}}$ mean: -24.2‰) and C:N ratio (mean: 15.8). The radiocarbon age at 72 cm in core 4 is 9180 \pm 110 Cal yrs BP. Multiple small fish vertebrae were preserved in the sediment, indicating that it is highly likely that an aquatic habitat existed in Palm Cave by this time (**Figure 6**). The benthic foraminiferal community has a low diversity ($H' = 0.6$) and species richness ($R = 3$), and is dominated by *Polysaccammina ipohalina* (mean: 69.6%) and *Tiphrotrocha comprimata* (mean: 28.1%). *Polysaccammina ipohalina* is known from freshwater-influenced high salt marshes areas and low salinity areas (Scott, 1976; Roe and Patterson, 2006). In Bermuda, this assemblage had not been observed in modern cave habitats (Cresswell and van Hengstum, 2021), but *P. ipohalina* has been observed in mangroves and ponds (Javaux and Scott, 2003).

4.3 High Oligohaline Assemblage (9230 to 8980 Years Ago)

The light brown sapropel also contained the high oligohaline assemblage, which includes foraminifera that are commonly found in slightly higher salinity settings. The high oligohaline assemblage is present in core 4 (52 to 71 cm) and core 10 (55 to 111 cm). The fine silt sediment (mean: 15.4 μm) is characterized by mostly terrestrially sourced organic carbon

TABLE 1 | Diversity table for sediment cores. Arithmetic mean of the relative abundance of dominant taxa and textural characteristic for each assemblage. Species with a mean of <1% relative abundance in the assemblage were marked with a dash to emphasize dominant individuals.

Assemblages	Saline groundwater	Meteoric Lens			Saline groundwater		
		Terrestrial Organic Carbon			Marine Organic Carbon		
	Subtidal <i>n</i> = 6	Low oligohaline <i>n</i> = 4	High oligohaline <i>n</i> = 17	Brackish <i>n</i> = 11	Lower TOC micrite <i>n</i> = 10	Higher TOC micrite <i>n</i> = 25	Carbonate mud <i>n</i> = 27
Approximate Time (Cal yrs BP)	9540 – 9480	9180 ± 110	9230 – 8980	8580	7000 – 1000		3610 – 720
Sediment Properties							
Coarse sediment (mg/cc)	4.3 ± 4.1	27.7 ± 26.4	15.4 ± 14.2	8.6 ± 6.6	18.2 ± 20.5	9.7 ± 14.3	52.7 ± 129.4
δ ¹³ C _{org}	-23.1 ± 1.6	-24.2 ± 0.4	-24.1 ± 0.8	-23 ± 0.3	-19.3 ± 2	-19.5 ± 1.3	-19.5 ± 1.1
C:N	15.7 ± 2.6	15.8 ± 0.6	15.6 ± 0.7	14.3 ± 0.7	11.6 ± 1.7	11.4 ± 1.6	10.3 ± 1
Terrestrial organic carbon (%)	62.8 ± 13.1	72.2 ± 3.5	71.3 ± 6.3	62.7 ± 2.6	32.5 ± 16.3	34.1 ± 10.6	33.8 ± 8.5
Total organic carbon (%)	19.3 ± 11	25 ± 5.9	24.2 ± 4.5	14.3 ± 3.6	2.2 ± 1.5	3.6 ± 1.6	6.7 ± 3
Foraminifera							
Total Individuals (cm-3)	355	85.8	197	168.4	5743.5	14021	9855
Shannon-Weiner Diversity (H)	2.30	0.60	0.40	1.00	2.40	2.60	3
Species Richness (R)	26.00	3.00	5.30	5.80	25.60	27.80	31
Relative Abundance							
<i>Bolivina</i> spp.	36.4	–	–	71.8	17.1	8.2	7.8
<i>Cibicides lobatulus</i>	3.6	–	–	–	1.4	–	2.8
<i>Cyclogyra involvens</i>	–	–	–	–	–	1.7	4
<i>Entzia macrescens</i>	–	1.3	3.2	4.3	–	–	–
<i>Globocassidulina subglobosa</i>	10.8	–	–	–	5.6	3.8	2.5
<i>Melonis barleeaanum</i>	3.4	–	–	–	1.9	–	2.6
<i>Miliolinella</i> spp.	–	–	–	–	1.2	4.3	7.3
<i>Patellina</i> spp.	1.2	–	–	–	1.1	13.5	5.5
<i>Polysaccammina ipohalina</i>	–	69.6	2.5	1.0	–	–	–
<i>Quinqueloculina</i> spp.	–	–	–	–	1.1	7.3	8.6
<i>Rosalina</i> spp.	15.1	–	–	8.1	7.9	7.0	7.7
<i>Rotallia</i> spp.	1.6	–	–	–	24.2	13.8	5.8
<i>Sigmolinita tenuis</i>	–	–	–	–	3.7	3.0	1.7
<i>Siphonina</i> spp.	2.7	–	–	–	2.5	–	1.3
<i>Spirillina vivipara</i>	–	–	–	–	1.4	11.1	8.9
<i>Spirophthalmidium emaciatum</i>	–	–	–	–	12.4	10.7	4.1
<i>Svratkina australiensis</i>	3.5	–	–	–	3.8	1.5	2.3
<i>Tiphotrocha comprimata</i>	2.4	28.1	90.6	9.8	–	–	–
<i>Triloculina</i> spp.	–	–	1.4	–	–	–	1.5
<i>Trochammina</i> spp.	–	–	–	–	2.8	–	5
<i>Tubenilla</i> spp.	–	–	–	–	–	2.8	6.8
Sum	99.4	100.0	99.9	99.9	99.3	99.6	98.9

(δ¹³C_{org} mean: -24.1‰; terrestrial organic carbon mean: 71.3%; total organic carbon mean: 24.2%). The age in core 4 at 60 cm is 8980 ± 50 Cal yrs BP and in core 10 at 110 cm is 9230 ± 100 Cal yrs BP. This very low diversity (*H* = 0.4) assemblage is a nearly uniform population of *Tiphotrocha comprimata* (mean: 90.6%), with a low relative abundance of *P. ipohalina* (mean: 2.5%) and *Entzia macrescens* (mean: 3.2%) (Table 1). These are all common taxa in low salinity (<5 psu) coastal environments in Bermuda and elsewhere (Javaux and Scott, 2003) (Scott, 1976). Outside of salt marshes, *Tiphotrocha comprimata* is a common benthic foraminifera in the sinkhole (i.e., cenote) El Eden on the Yucatan Peninsula, which has a salinity of ~3.5 psu (misidentified as *Tritaxis* by van Hengstum et al., 2008).

4.4 Brackish Assemblage (8580 yrs BP)

The brackish assemblage is present in core 4 (35 to 47 cm) and in core 10 (25 to 35 cm) at the top of the light brown sapropel, which is characterized by fine silt (mean: 8.6 μm) and organic carbon derived from primarily terrestrial sources (δ¹³C_{org} mean: -23 ‰; total organic carbon mean 14.3%). The radiocarbon date in core 4 at 32 cm was aged at 8480 ± 60 Cal yrs BP. This assemblage is characterized by increased foraminiferal diversity and species richness (*H* = 1), and dominated by the infaunal biserial taxa *Bolivina* spp. (mean: 71.8%) and the epifaunal rotaliid *Rosalina* spp. (mean: 8.1%). The relative abundance of *T. comprimata* is less than in the oligohaline-inferred assemblages (mean: 9.8%; Table 6). It is important to note that *Rosalina* is present in this assemblage, but not in the previously described oligohaline

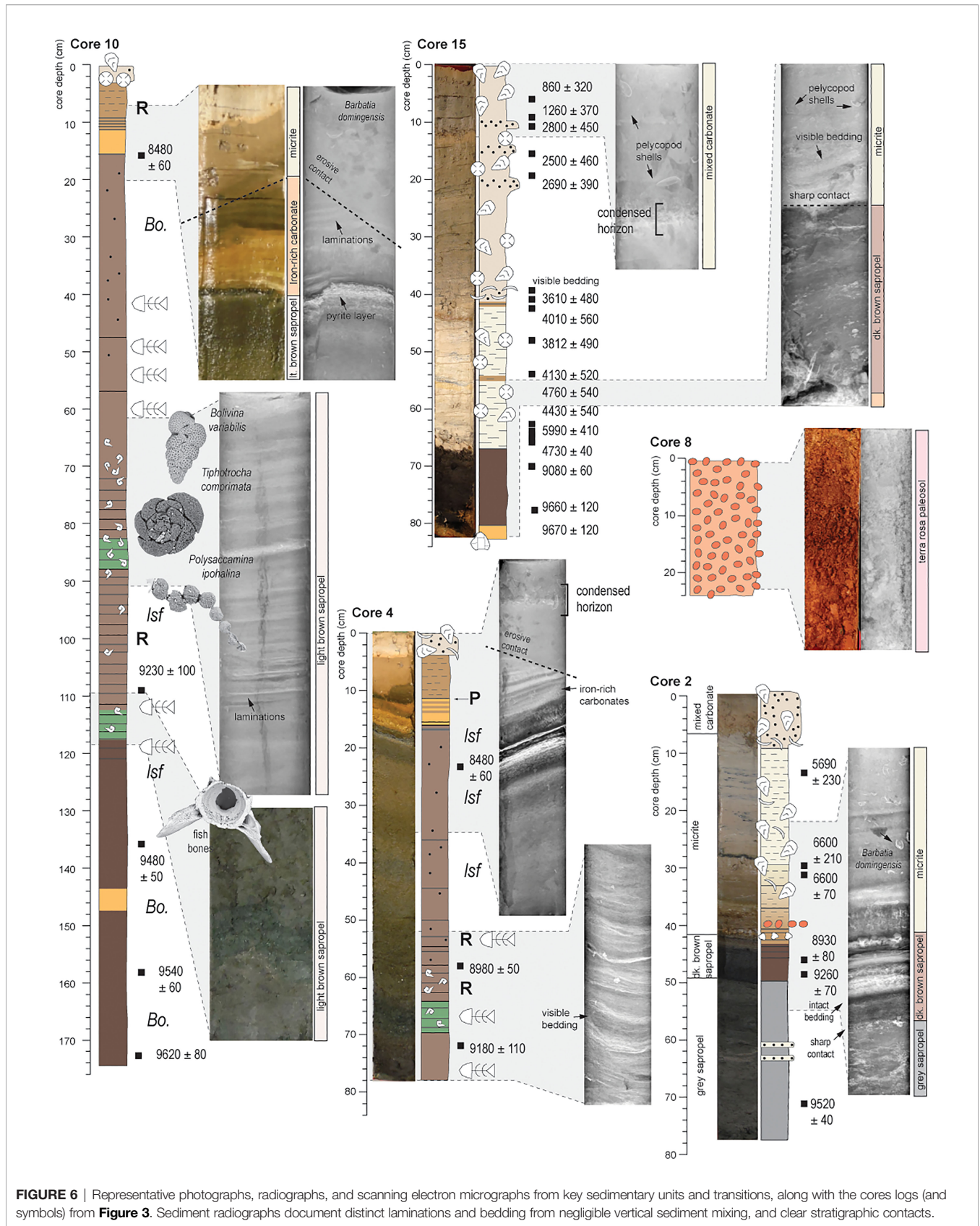


FIGURE 6 | Representative photographs, radiographs, and scanning electron micrographs from key sedimentary units and transitions, along with the cores logs (and symbols) from **Figure 3**. Sediment radiographs document distinct laminations and bedding from negligible vertical sediment mixing, and clear stratigraphic contacts.

assemblages. This indicates that the *Bolivina* spp. cannot simply be explained by younger-aged *Bolivina* individuals burrowing into pre-existing and older sediment, but rather the *Bolivina* and *Rosalina* were co-occurring as part of a unique assemblage of foraminifera. It is also worth noting that this assemblage did not contain other hyaline foraminifera (e.g., *Globocassidulina*). While both *Rosalina* and *Bolivina* are present in modern brackish settings in Bermudian anchialine environments (Cresswell and van Hengstum, 2021), they do not form a similar co-dominated assemblage in the modern environment and they individually are not diagnostic of a specific salinity range.

4.5 Lower TOC Micrite Assemblage (~7000 to ~1000 Years Ago)

The lower TOC micrite assemblage is present in the oldest micrite-dominated sediment, and it has a slightly lower TOC content $2.2 \pm 1.5\%$. The foraminiferal assemblage is dominated by *Rotalliella* spp. (mean: 24.2%), *Bolivina* spp. (mean: 17.1%), *Spirophthalmidium emaciatum* (mean: 12.4%) and other rotaliid taxa in lesser relative abundances (e.g., *Svatkina*, *Globocassidulina*, *Rosalina*, and *Cibicides*). The sediment is medium silt (mean: 18.2 μm) and has an enriched stable carbon isotope value of the bulk organic matter ($\delta^{13}\text{C}_{\text{org}}$ mean: -19.3‰ ; C:N ratio mean: 11.6). The assemblage is more diverse than sapropel assemblages ($H' = 2.4$). Based on the stratigraphic positions and constraining radiocarbon dates in multiple cores (Figure 3), it can be assumed that this assemblage existed from 7000 years ago (e.g., C2). However, it could have persisted in some cave locations until as recent as 1000 years ago (e.g., C7, C9) along with micrite deposition. The common marine taxa present within this assemblage suggests marine conditions were established at this time (Table 6). In Bermuda, *Spirophthalmidium emaciatum* is known to colonize cave areas that (i) are flooded by oxygenated saline groundwater, and achieve highest proportional abundances in areas that are distal to direct connections with adjacent coastal environments (van Hengstum and Scott, 2011), and (ii) have accumulating carbonate sediment with lower TOC concentrations (Cresswell and van Hengstum, 2021). This taxa also occurs elsewhere, including carbonate sediment in marine caves flooded by oxygenated saline groundwater in Spain (Bergamin et al., 2020) and Cozumel (Brankovits et al., 2021). Outside of caves in Bermuda (van Hengstum and Scott, 2012), *Rotalliella* is known in the deep-sea at 1980 mbsl on the Lomonosov Ridge off northeast Greenland (Scott and Vilks, 1991) and at 4450 mbsl on the Bermuda Rise in the Sargasso Sea (Pawlowski, 1991). *Spirophthalmidium* (identified as 'Spirirolucina sp.' was also observed in deep-sea sediment cores (4256 m deep) from the Sargasso Sea (see images 15-16 in Plate 5 in Phleger et al., 1953).

4.6 Higher TOC Micrite Assemblage (~7000 to ~1000 Years Ago)

The higher TOC micrite assemblage is associated with a subtly higher TOC content (mean: $3.6 \pm 1.6\%$) and is more diverse ($H' = 2.6$) than the lower TOC micrite assemblage, yet still occurs in sediment that is currently measured as fine carbonate silt (mean particle diameter: 9.7 μm). The assemblage is present in core 2 (12 to 32 cm), core 14 (8 to 28 cm), and core 15 (43 to 66 cm), and is

associated with an estimated 32.5% marine-derived organic carbon based on $\delta^{13}\text{C}_{\text{org}}$ values (mean: -19.5‰ ; C:N ratio mean: 11.4) with a TOC content of 2.2%. Age-bracketing radiocarbon results in from core 2 (32 and 12 cm) and core 15 (43, 50, 55, and 65 cm) indicate that this assemblage was deposited between 6600 ± 70 to 3812 ± 490 Cal yrs BP; a duration of ~ 2800 years. Taxonomically, *Rotalliella* spp. (mean: 13.8%) remains dominant, but the relative abundance of *Patellina* (mean: 13.5%) and *Spirillina vivipara* (mean: 11.1%) notably increase to similar values. According to Murray (2006), *Spirillina* and *Patellina* are known colonizers of hard substrates (i.e., rocks, shells) on continental shelves (<100 m), yet they are also found in the fine grained carbonate sediment on the cave benthos. This suggests that perhaps *Spirillina* and *Patellina* were originally living attached to the cave wall, and only became detached and part of the sediment record after death.

4.7 Carbonate Mud Assemblage (~4000 Years Ago to Present)

The radiocarbon ages from core 7 (10 cm & 60 cm) and core 15 (6, 10, 14, 20, 39, and 40 cm) indicate that the carbonate mud assemblage started accumulating in Palm Cave by 3610 ± 480 Cal yrs BP. However, the carbonate mud unit in the cores is the topmost and thinnest unit, so this unit has the greatest time averaging, least temporal resolution, and minimal power to preserve detailed environmental changes that have occurred in Palm Cave during the last 4000 years. This assemblage was found in a coarser textured substrate with a mean TOC content of $6.7 \pm 3.0\%$. The samples associated with this assemblage were from core 2 (4 to 8 cm), core 14 (4 to 6 cm), core 15 (4 to 42 cm), and core 7 (10 to 60 cm). The organic matter had a primarily marine provenance (Table 1). This was the most diverse assemblage observed in the stratigraphy ($H' = 3$), but it remained dominated by *Spirillina vivipara* (mean: 8.9%), *Quinqueloculina* spp. (mean: 8.6%), *Bolivina* spp. (mean: 7.8%), and *Rosalina* spp. (mean: 7.7%; Table 6). However, lower abundances of common marine cave taxa like *Spirophthalmidium emaciatum*, *Rotalliella*, and *Sigmoilina tenuis* could still be observed throughout.

5 DISCUSSION

5.1 Sea-Level Flooding and Anchialine Habitat Genesis

From first principles (Richards et al., 1994; Shinn et al., 1996; van Hengstum and Scott, 2011; Gregory et al., 2017), the floor of Palm Cave at 23 mbsl should have been flooded by the vertically-rising aquifer system in response to sea-level rise by 9,500 Cal yrs BP (Figure 7). Not all caves have accumulated sediment records, which is the result of multiple sedimentary, hydrologic, and geometric processes that operate caves (Kitamura et al., 2007; Fornós et al., 2009; Fornós et al., 2014; Collins et al., 2015; Kovacs et al., 2018). However, cave stratigraphy can provide a *minimum* age for when aquatic habitats formed as part of the karst subterranean estuary (van Hengstum et al., 2015). This is because the proxy requires favorable sedimentary and biologic processes to leave a stratigraphic record of this event. For

example, sedimentation may not initiate with cave floor flooding or anytime thereafter (Fornós et al., 2009), cave sediment supply may be linked to changes in adjacent coastal and terrestrial environments (Collins et al., 2015; Gregory et al., 2017), or sediment may be reworked and transported out of a cave by groundwater currents or extreme rainfall events (Brankovits et al., 2021).

Basal organic-rich sedimentary deposits dated cores 10, 14, and 15 from Palm Cave are very closely aged to the expected timing of cave floor inundation by concomitant sea-level and groundwater rise during the middle Holocene (~9,800 years, within dating uncertainties). Vollbrecht (1996) completed an extensive marine geological investigation of Harrington Sound, which included radiocarbon dating multiple basal peat samples in contact with carbonate lithology. While there is some uncertainty on whether these basal peats were derived from a freshwater or terrestrial origin, the resultant database can still be considered a compilation of terrestrial limiting sea-level indicators (Hijma et al., 2015) (Figure 7). Overall, this database agrees very well with modeled estimates for relative sea-level rise in Bermuda (Love et al., 2016) after considering glacioisostatic adjustment of the eastern North American plate from Laurentide Ice Sheet melting (Figure 7). It is highly likely that both the continuity of a subtropical forest above Palm Cave and its inherited 7 separate entrances ensured both (i) a constant source of organic-based sediment for transport, and (ii) continual point sources for sediment to enter the cave (Figure 2). In fact, there is an entrance very proximal to the precise location where these oldest sediments were accumulating (Figure 2), and deposition would have been minimally impacted by complex horizontal cave transport and baffling effects from undulating cave ceilings (as per Collins et al., 2015). Given the amount of organic matter in the stratigraphy (i.e., C10), however, we cannot rule-out that there was once a deeper cave tunnel (now filled in with sediment) that once connected the southern part of Palm Cave to the outside surface when wetlands colonized the proximal area in the early Holocene (Figure 2, Vollbrecht, 1996).

It is equally important that the organic-rich sapropel contained benthic meiofaunal remains (e.g., foraminifera and ostracodes), which preserved evidence of the physicochemical conditions of the paleo groundwater conditions during initial flooding. Calcite rafts were observed sporadically throughout the light brown sapropel, but they did not form a distinctive sediment layer or constituent like elsewhere in Bermuda (van Hengstum et al., 2011) and Mexico (Kovacs et al., 2017). Sediment from the grey sapropel notably did not contain benthic foraminifera, just freshwater ostracodes like *Darwinula stevensoni* or *Cypridopsis vidua* (Keyser, 1977; Williams and Williams, 1998; Keyser and Schöning, 2000). In contrast, the dark brown sapropel at the base of C10 contained an assemblage of foraminifera dominated by *Bolivina* spp. (mean: 36.4%), and epifaunal rotaliids such as *Rosalina* spp. (mean: 15.1%), *Globocassidulina subglobosa* (mean 10.8%), and *Svratkina australiensis* (mean: 3.5%; Table 6). In modern Bermudian anchialine settings, this foraminiferal assemblage is similar to

fauna observed in total assemblages from shallow, subtidal habitats influenced by abundant particulate organic flux from the terrestrial landscape (Little and van Hengstum, 2019; Cresswell and van Hengstum, 2021). In a fossil setting, a similar assemblage was found in southern England that likely reflects analogous fossil anchialine conditions related to previous interglacial sea-level highstands during the late Pleistocene (Proctor and Smart, 1991). Problematically, both the dark brown sapropel containing foraminifera (subtidal assemblage) and the grey-hued sapropel containing ostracods like *Darwinula stevensoni* or *Cypridopsis vidua* were accumulating in Palm Cave at nearly the same time. The fact that they are slightly different sedimentary units with different meiofaunal remains indicates that some time-transgressive environmental changes in the cave benthos likely occurred. Precisely resolving the timing for the emplacement of these separate sedimentary deposits is limited by the uncertainty on the radiocarbon dates available and the dating method itself. For example, basal sediments in C14 (9750 ± 210, grey sapropel) and C10 (9620 ± 80, dark brown sapropel) have overlapping ages at the 95% confidence level (2σ), and would require better preserved terrestrial plant macrofossils in additional core samples to resolve these dating uncertainties that span several centuries. Nevertheless, within a few hundred years, Palm Cave was flooded by a rising meteoric lens of a coastal aquifer, which likely first triggered oligohaline benthic anchialine environmental conditions.

It is also noteworthy that an intertidal assemblage of benthic foraminifera was not preserved in the stratigraphy of Palm Cave. Using recent foraminiferal assemblages, Little and van Hengstum (2019) documented a unique intertidal assemblage of foraminifera at the entrance to Cow Cave that was dominated by *Trochammina inflata*, *Milimmina fusca*, *Triloculina oblonga*, and *Entzia macrescens*. While the site of Palm Cave would have been positioned slightly more distal to the shoreline during its initial inundation by the coastal aquifer, tidal oscillations of the groundwater table can still be observed 10² kms inland on porous carbonate platforms (Coutino et al., 2021). It is possible that intertidal conditions were too short-lived and the sedimentation rate too low in Palm Cave at initial inundation for the sediment record to archive this event. Alternatively, perhaps another ecological parameter precluded colonization of *Trochammina inflata* and *Milimmina fusca* during the early aquatic history of Palm Cave.

5.2 The Paleo Meteoric Lens and Associated Brackish Conditions: 9300 to 8400 Cal yrs BP

By 9200 years ago, distinctive and separate foraminiferal assemblages can be identified in the light brown sapropel that can be associated with a paleo meteoric lens flooding the benthic habitats in Palm Cave. Overall, the foraminiferal assemblages are dominated by *Polysaccamina ipohalina*, *Tiphotrocha comprimata*, and *Entzia macrescens*, which are commonly known in oligohaline and brackish water settings (previously introduced). At a Bray-Curtis dissimilarity index of 0.5, the assemblages can be divided into a low oligohaline, high

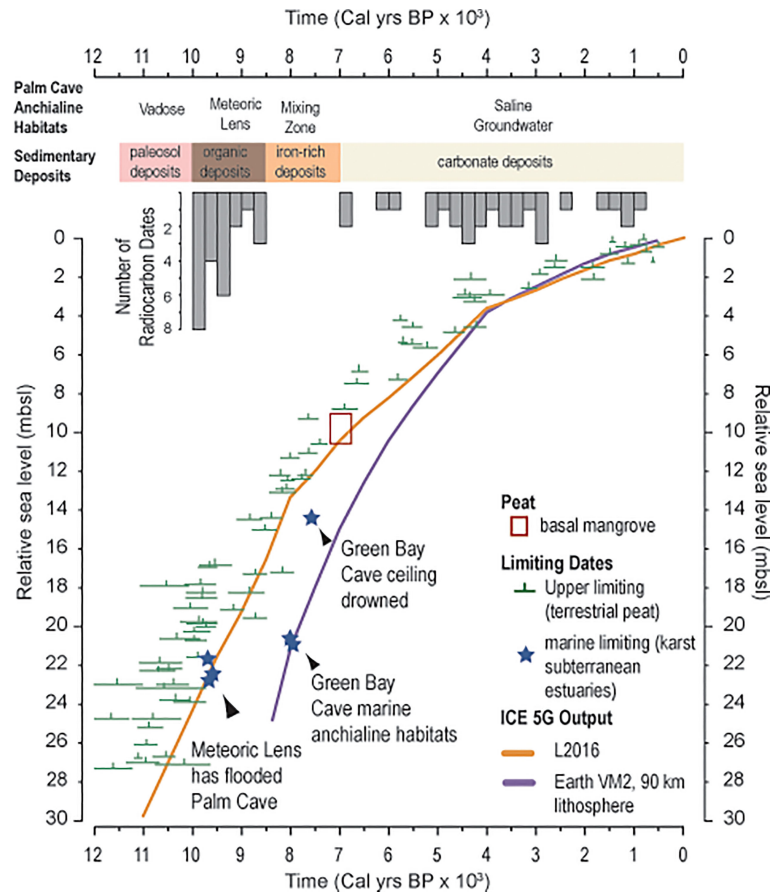


FIGURE 7 | A database of upper limiting sea level indicators from Bermuda cores is compared two glacial isostatic adjustment models, purple line is ICE-5G (Peltier, 2004) and orange line is L2016 (Love et al., 2016). The top of the meteoric lens qualifies as a marine limiting sea level indicator, which is estimated from Palm Cave by the radiocarbon age of sediment above the limestone in the cave that contains evidence of microfossils documenting the onset of aquatic conditions of the cave. While the Palm Cave data agrees well with expectations of the position of sea level, sedimentation in Green Bay Cave was delayed by several millennia after it was initially flooded by a meteoric lens.

oligohaline and brackish assemblage, depending on the relative dominance of these three species. Given uncertainties in radiocarbon dating, however, it cannot be ruled out that both the low and high oligohaline assemblages were co-occurring from ~9300 to 8900 years ago, whereby benthic salinity during this period was confidently less than 5 psu and resident foraminiferal populations just oscillated between dominant taxa, or some taphonomic bias alternatively favored preservation of one taxa. At Cenote El Eden (20.491, -87.258), which is located ~1400 m from the eastern Yucatan Peninsula shoreline, the local meteoric lens is oligohaline (>3.3 psu) (van Hengstum et al., 2008). Cenote El Eden hosts a population of *Tiphrotrocha comprimata* (mean proportion: 21%) and *Ammonia* (mean proportion: 51%). The conditions in Cenote El Eden provide a modern analog for the possible benthic salinity and overlying water column in Palm Cave from ~9300 to 8400 years ago.

At 8500 years ago, the benthic foraminiferal diversity increases and is characterized by a significant increase of *Bolivina* spp. (71.8%), *Rosalina* spp. (8.1%), *Entzia macrescens* (4.3%), while the proportional abundance of *T. comprimata*

(9.8%) and *P. ipohalina* (1%) decrease. However, we do not observe the occurrence of calcareous taxa such as *Melonis*, *Globocassidulina*, or *Svratkina* (Figure 4), which Little and van Hengstum (2019) observed as primarily in subtidal benthic habitats flooded by saline groundwater in Bermuda. The presence of *Bolivina* and *Rosalina* are not salinity-diagnostic, but they are known to tolerate brackish areas in modern caves and sinkholes (Cresswell and van Hengstum, 2021). Taken collectively, the increasing proportion of calcareous individuals (e.g., *Bolivina*, *Rosalina*) suggests that salinity increased from oligohaline to higher brackish conditions in a local paleo meteoric lens from 9300 to 8400 years ago.

During the period of initial cave inundation and deposition of the organic-rich facies, the particulate organic carbon (POC) had primarily depleted stable carbon isotopic ratios. For example, the dark brown sapropel had a $\delta^{13}\text{C}_{\text{org}}$ value of $-24.1 \pm 0.9\text{‰}$ and a C:N ratio of 16.8 ± 1.1 ($n = 43$), which would suggest that the POC had a primarily terrestrial origin. However, as the cave gradually flooded with groundwater, it is likely that some primary productivity was occurring in a paleo meteoric lens

around the cave openings, as these areas would have received some indirect light. If true, the benthos could have been supplied by organic matter from both primary productivity and the forest landscape above. Given the overlapping numerical range of $\delta^{13}\text{C}_{\text{org}}$ POC from fresh to brackish primary productivity and terrestrial POC, the C:N ratio can help inform POC sourcing since phytoplankton remains contribute higher nitrogen content to the sediment record (Lamb et al., 2006; van Hengstum et al., 2010; Tamalavage et al., 2018). While both the $\delta^{13}\text{C}_{\text{org}}$ value and C:N ratio of the light brown sapropel (C:N: 14.9 ± 1.1 , $\delta^{13}\text{C}_{\text{org}}$: $-23.5 \pm 0.9\text{‰}$, $n = 39$) is within uncertainty of the dark brown sapropel, the C:N ratio of the light brown sapropel exhibits a distinctly greater range of C:N ratio values to a minimum of almost 10 (Figure 3). This result is consistent with the light brown sapropel receiving some contribution of phytoplankton POC versus the dark brown sapropel from primary productivity around Palm Cave entrances. These inferences would also explain why stratigraphic levels in C10 have a greenish hue from increased proportion of pelagic-based POC, and an expanded pelagic ecosystem explains why small fish vertebrae were regularly observed in the light brown sapropel unit (Figure 6). It cannot be ruled out that the increased proportion of *Rosalina* and *Bolivina* in the brackish assemblage was driven by increased benthic delivery of more labile organic carbonate relative to the low and high oligohaline assemblages. Nevertheless, the combined results indicate that the cave was still flooded by a paleo meteoric lens during deposition of all the organic-rich sedimentary units.

5.3 Iron-Rich Carbonate Deposition: ~8400 to ~7000 Cal yrs BP

Iron-rich carbonate deposition was initiated at 8480 ± 60 Cal yrs BP based on the radiocarbon result in C10, and it ceased by ~7000 years ago based on the radiocarbon dates from C2. This interval of time is marked by a sedimentary hiatus in many cores (disconformity, examples: C3, C6), but in C10 and C4 there is a distinct layer of orange-hued, carbonate-rich sediment. There is also iron-rich carbonates towards the base of C10, and above the limestone in C15. Negligible foraminifera were noted, only the rare low-oxic tolerant *Bolivina* spp. were observed. However, the infaunal *Bolivina* could also be preserved at this stratigraphic elevation by colonizing the iron-rich substrate when favorable physiochemical conditions returned to the sediment-water interface, since there were no co-occurring epifaunal taxa in the iron-rich carbonate unit (e.g., *Rosalina*). Previous research has shown oxidative precipitation of dissolved Fe (II) from the mixing of seawater and groundwater generates a distinctive increase in iron oxide deposits in the subsurface zone (Charette & Sholkovitz, 2002). This process is driven by pH gradients between the anoxic saline versus oxygenated freshwater above (Spiteri, et al., 2006), and the iron curtain can spatially migrate in response to sea level change (Roy et al., 2010). Geochemical processes occurring in the iron curtain have been an important driver for increased research on 'subterranean estuaries' on siliciclastic coastlines, but an active iron curtain has yet to be documented in karst subterranean estuaries.

We forward the hypothesis that the iron-rich carbonate deposits result from the upwelling of anoxic saline groundwater through the limestone, which promotes the rapid precipitation of dissolved Fe (II) when the anoxic saline groundwater hits the oxygenated cave layer. As previously presented, we posit that the cave was first flooded by a meteoric lens. With continued sea-level rise, however, the pycnocline between the saline groundwater and the meteoric lens would have eventually become proximal to the sediment-water interface, in turn promoting oxidative precipitation of iron oxide. Indeed, the stratigraphic architecture of C15 (67-82 cm) is perhaps contrary to this environmental change sequence with groundwater-level rise, namely inverted basal iron-rich carbonates followed by dark brown sapropel (Figure 3). But given the research design, it cannot be ruled out that the older dark brown sapropel sediment preserved at C15 was re-worked from elsewhere in the cave at a younger point in time. While negligible iron concentrations were detected in water samples across the expansive karst subterranean estuaries of the Yucatan Peninsula (Gonneea et al., 2014), perhaps the sedimentary observations from Palm Cave in Bermuda are indicating that the iron is becoming baffled in subsurface porosity like horizontally expansive caves.

5.4 POC Flux Changes from Groundwater Circulation and Cave Geometry During Saline Groundwater Conditions

The carbonate stratigraphy in Palm Cave can be notably divided into two units: (i) an older and finer-grained micritic unit that is notable whiter-hued, more dense, and has common remains of the bivalve *Barbatia domingensis*, versus (ii) a mixed carbonate mud that is coarser in texture and typically contains abundant invertebrate remains. Indeed, a *sensu stricto* definition of micrite is sedimentary particles <4 μm in diameter, but on millennial timescales, it is very likely that the original carbonate particles experienced some aggregation from subsurface fluid migration, diagenesis and clumping. In a modern location in Bermuda, micrite is currently accumulating in areas of Cow Cave flooded by <1 m of water depth and no direct connection to the sea (Little and van Hengstum, 2019). The carbonate units, both the micrite and mixed carbonate unit, had organic matter that is markedly similar in its estimate of a marine provenance 32-34% and includes both what is produced *in situ* and the POC transported from outside the cave (Table 1). However, there are notable differences in TOC content, sedimentary texture, and foraminifera that indicate they were accumulating under different environmental conditions.

The final primary environmental change occurred in Palm Cave when it was definitively flooded by oxygenated saline groundwater, which was prior to 6600 ± 70 Cal yrs BP based on the radiocarbon dates at 35 cm in C2. The onset of marine conditions allowed invertebrates like bivalves (e.g., *Barbatia domingensis*), bryozoans (*Cheilostomata*), coral (*Coenocyathus goreau*), brachiopods, marine ostracodes to colonize, and the diversity of the benthic foraminifera significantly increased. This also coincided with widespread micrite deposition throughout

Palm Cave. But, the micrite unit contained evidence of two separate foraminiferal assemblages: a lower diversity ($H' = 2.6$, TOC: $2.2 \pm 1.5\%$, cores C10, C4, few samples from C2, C7) versus a higher diversity ($H' = 2.6$, TOC: $3.6 \pm 1.6\%$; cores C15, C2, and C14) assemblage. For example, the high TOC micrite assemblage had >53% of just *Spirophthalmidium*, *Rotaliella*, and *Bolivina*, whereas the younger low TOC assemblage was >38% *Rotaliella*, *Patellina*, and *Spirillina* along with increased species richness. Palm Cave does not have a large, submarine cave opening like Green Bay Cave in Bermuda, so any groundwater changes must have been translated through the host lithology and smaller porosity by saline groundwater circulation. The large range in $\delta^{13}\text{C}_{\text{org}}$ values in the micrite unit as whole likely reflect the variability of terrestrial POC that could have still entered the cave through the 7 cave openings to the subtropical forest above. The youngest assemblage to characterize the benthic cave habitat was the carbonate mud assemblage, which had the highest diversity, coarsest textured substrate, and highest mean TOC content ($6.7 \pm 3.0\%$) and range.

During the period from 7000 to 3000 years ago, these marine-based foraminiferal assemblages are co-occurring in Palm Cave, but their location is spatially variable and they do not exhibit cave-wide time dependent turn over events. While we did not analyze benthic foraminifera in every stratigraphic level in the cores and the possibility of hiatus between cores is likely, the stratigraphy suggests that cessation of micrite deposition is variable throughout Palm Cave (~1000 years ago in C9, ~2600 years ago in C12, and ~3600 years ago in C2) at similar depths. This rules-out that water table elevational changes alone were the sole driver of benthic habitat variability after Palm Cave become flooded by oxygenated saline groundwater.

In Bermuda's flooded that are currently flooded by oxygenated saline groundwater, recent benthic foraminiferal distributions exhibit spatial variability from POC quantity and source delivered to the sediment-water interface (Cresswell and van Hengstum, 2021). For example, the diversity of foraminiferal assemblages decreases with increasing distance away from the primary marine entrance in Green Bay Cave (van Hengstum and Scott, 2011). Foraminiferal assemblages most distal from cave openings are most dependent on passive nutrient delivery by circulating saline groundwater, and are dominated by *Spirophthalmidium*, *Rotaliella*, *Patellina*, and *Spirillina*. Previously, we suggested that *S. emaciatum* was a dominant taxa in the most oligotrophic conditions, where it is not outcompeted by other lagoonal taxa like miliolids (van Hengstum & Scott, 2011). Elsewhere, Brankovits et al. (2021) also documented how the POC quantity and source can drive community shifts in benthic foraminifera living in the passages of Aerolito Cave (Cozumel, Mexico) that are flooded by oxygenated saline groundwater. Similarly, others have documented changes in the flux and supply of POC and its impact on benthic habitat variability and ecosystems in Mediterranean submarine caves (Fichez, 1991b; Fichez, 1991a). The spatial variability of benthic foraminiferal assemblages in Palm Cave during the marine phase is consistent with these modern observations in both the Atlantic and Mediterranean realms. The low vs. high TOC micrite assemblages (section 4.5

and 4.6 above) may simply reflect intervals when that particular cave location received more vs. less POC delivery, as supported by the TOC measurements, combined with favorable hydrologic conditions for micrite precipitation and accumulation.

Holocene environmental change in Palm Cave must also be considered relative to subaerial flooded of the Bermuda carbonate platform, especially since many flooded cave entrances are located on the periphery of Harrington Sound. In general, broadscale groundwater salinity changes in Palm Cave are strikingly similar to the aquatic development in Harrington Sound in response to Holocene sea-level rise. From ~9400 to ~7000 years ago, Harrington Sound hosted a fresh to brackish water pond, whose shoreline was <50 m from Palm Cave through the limestone rock, and this supported the potential for a meteoric lens to be flooding Palm Cave. By ~7000 years ago, continual flooding by Holocene sea-level rise had transitioned Harrington Sound into a restricted marine pond (Vollbrecht, 1996), and environmental conditions in Palm Cave similarly became marine as the cave became flooded by oxygenated saline groundwater [see Abb. 25 in (Vollbrecht, 1996)].

A final shift in benthic foraminiferal taxa is observed in the carbonate mud assemblage, which was the most diverse ($H = 3$) and occurred in the coarsest substrate. The dominant marine taxa include *Spirillina vivipara*, *Patellina* spp., *Miliolinella* spp., and *Quinqueloculina* spp. with lower abundance of *Spirophthalmidium emaciatum*. Samples associated with this assemblage appear consistently younger than ~4000 years based on radiocarbon dates in C15 at the contact between micrite and carbonate mud (3610 ± 480 Cal yrs BP, 4010 ± 560 Cal yrs BP). In the modern setting, considerable tidal currents develop in Palm Cave along eastern passages, and are likely associated with enhanced tidal exchange of seawater between the subsurface and Harrington Sound through Cripplegate (**Figure 2**), and perhaps an additional (i.e., unmapped) favorable hydrologic pathway in the southern part of Palm Cave. It is highly likely that the final transition to the high diversity carbonate mud assemblage was initiated by higher (i.e., modern-like) groundwater flow velocities in the cave, which perhaps was linked to regional changes in seawater circulation in Harrington Sound. Increased groundwater flow would favor accumulation of a coarser substrate, since fine micrite particles would be winnowed away. Consistent with measurements of higher TOC in the carbonate mud assemblage, increased groundwater currents would potentially enhance POC delivery throughout the cave, in turn promoting the observed higher diversity foraminiferal assemblages in the last ~4000 years.

5.5 Broader Implications and Limitations

The new results from Palm Cave also help refine interpretations of paleo environmental change and sedimentation in other Bermudian underwater caves. Based on the evidence from Palm Cave, the water table of the coastal aquifer was positioned 23 mbsl at ~9800 years ago. In nearby Green Bay Cave, however, sedimentation at 20.7 ± 0.8 mbsl did not initiate until 7720 ± 120 Cal yrs BP at the site of C11 or 7690 ± 150 Cal yrs BP at the site of C15 (see Figures 8, 9 in van Hengstum et al., 2011). Based on the modeled relative sea-level curve that is validated by available field data (**Figure 7**), the water table should

have flooded the floor of GBC at ~21 mbsl by ~9200 years ago. By corollary and simple arithmetic, it can be inferred that the core site of C11 in Green Bay Cave was already flooded by >5 m of groundwater by ~7700 years ago. As discussed by Collins et al. (2015), the onset of sedimentation in Green Bay Cave was delayed for several millennium after inundation by the rising coastal aquifer. Sedimentation was only initiated in Green Bay Cave when the groundwater column became geochemically suitable for both *in situ* carbonate precipitation (both calcite rafts and micrite) and benthic habitats were suitable for marine benthic foraminifera. Such prehistoric conditions are perhaps geochemically similar to the modern environmental conditions in Cow Cave, wherein micrite is currently precipitating (Little and van Hengstum, 2019). While it is beyond the scope of the present work, our understanding of inferred paleo meteoric lens behavior in the Harrington Sound area (van Hengstum and Scott, 2012) needs revision given (i) the improved understanding of Holocene groundwater elevation and salinity changes in Bermuda (discussed further below) and (ii) the significant improvement in knowledge of underwater cave and sinkhole sedimentology over the last decade.

Modern Bermudian caves like Palm Cave and Green Bay Cave are populated by the endemic anchialine marine shrimps *Procaris chacei* (Hart and Manning, 1986) and *Typhlata iliffei* (Hunter et al., 2007), which currently live in oxygenated saline groundwater. Thus, these marine shrimps could not have been occupying Palm Cave from 9200 to 8400 years ago when it was flooded by an oligohaline meteoric lens, and they must have migrated into Palm Cave from the platform below at a younger time. The benthic foraminiferal evidence indicates that these marine crustaceans could have colonized Palm Cave no sooner than ~7000 years ago, and migrated into Palm Cave as it become flooded with saline groundwater as subsurface marine anchialine habitats expanded (van Hengstum et al., 2019).

An important caveat to the results presented here is that the anchialine environments commonly investigated in Bermuda (e.g., Green Bay Cave, Palm Cave, Walsingham, Leamington) are currently flooded by well-oxygenated saline groundwater owing to (i) their shoreline proximity, (ii) tidally-forced subsurface currents, and (iii) direct physical openings to adjacent marine lagoons. An analogous setting occurs in shoreline proximal areas of Aerolito Cave in Cozumel in Mexico (Mejía-Ortiz et al., 2007; Brankovits et al., 2021). Ecosystem process and fauna from Bermudian anchialine environments can only be compared globally in that hydrographic context. It is well understood that dissolved oxygen concentrations in the saline groundwater mass rapidly decrease when the geomorphologic and hydrographic conditions described above do not exist, which will necessarily exert additional environmental pressure and promote further spatial benthic habitat variability. In their current hydrogeological configuration, the commonly-explored caves in Bermuda are not suitable for investigating how lowered dissolved oxygen concentrations impacted modern habitat variability (either benthic or pelagic). If this information can be derived elsewhere, however, it would be helpful for interpreting subfossil foraminifera preserved in cave stratigraphy.

6 CONCLUSIONS

Palm Cave preserves the best known stratigraphic and microfossil record yet known from an anchialine environment flooded by a karst subterranean estuary. Over the last 9500 years, benthic habitats in Palm Cave were primarily controlled by the vertically migrating coastal aquifer in response to deglacial sea-level rise. The vertical passage of the primary groundwater masses in the coastal aquifer—the meteoric lens and saline groundwater—was recorded by the cave stratigraphy and preserved meiofaunal remains. In turn, the individual groundwater masses controlled salinity in the water column and dictated the primary ecological boundary condition for aquatic ecosystems owing to osmotic-forcing. Similar to other authors [see **Figure 2** in (Chávez-Solís et al., 2020) or **Figure 5** in Ballou et al. 2022], this work demonstrates the importance of considering and comparing modern anchialine organisms to others that exist in specific water masses to better inform both ecosystem and evolutionary processes. Once a specific groundwater mass was emplaced, the benthic foraminiferal assemblages secondarily responded to the source and quantity of POC supplied to the sediment-water interface. This included (i) a likely favorable response to an increased POC flux from N-rich phytoplankton tissues during the older meteoric lens phase of the cave history, and (ii) increased POC delivery by groundwater circulation and currents during the younger saline groundwater mass phase. In instances where dissolved oxygen concentrations in the groundwater is not an ecologically limiting factor, salinity and POC source and quantity exert a fundamental control on benthic habitat variability in anchialine environments.

The stratigraphic architecture of Palm Cave includes an iron-rich sedimentary unit that is anomalous within its current hydrogeologic context (i.e., well-oxygenated saline groundwater). The age of the sedimentary unit is after the cave was flooded by an oxygenated meteoric lens. These sedimentary deposits have also been observed elsewhere in the stratigraphic record of Bermuda's caves (van Hengstum et al., 2011). We hypothesize that these iron-rich sediments were deposited by upwelling anoxic saline groundwater through the karst, and oxidative precipitation of iron occurred as anoxic seawater encountered oxygenated water cave passages, similar to the well-documented processes related to 'iron curtains' located proximal to the shoreline in siliciclastic subterranean estuaries (Charette and Sholkovitz, 2002). While modern groundwater masses in karst subterranean estuaries have low dissolved iron concentrations (Gonneea et al., 2014), perhaps it is warranted to re-evaluate where and when the 'iron curtain' occurs on karst landscapes.

DATA AVAILABILITY STATEMENT

The original contributions presented in the study are included in the article/**Supplementary Material**. Further inquiries can be directed to the corresponding author.

AUTHOR CONTRIBUTIONS

PvH designed the research and collected the core samples, JC completed laboratory activities, PvH and JC jointly interpreted that data, generated the artwork, and co-wrote the final manuscript. All authors contributed to the article and approved the submitted version.

FUNDING

Funding for this research was provided by the resources supplied to TAMUG from the Texas Institute of Oceanography (JC), NSF Awards (OCE-1519557, EAR-1703087), the 2016 Kathy Johnston Scholarship from the American Academy of Underwater Sciences, student research grants to JC from the Geological Society of America.

REFERENCES

- Ballou, L., Brankovits, D., Chávez-Solís, E.M., Gonzalez, B. C., Rohret, S., Salinas, A. et al. (2022). An Integrative Re-Evaluation of Typhlatya Shrimp Within the Karst Aquifer of the Yucatán Peninsula, Mexico. *Sci Rep.* 12, 5302. doi: 10.1038/s41598-022-08779-9
- Bates, N. R. (2017). Twenty Years of Marine Carbon Cycle Observations at Devils Hole Bermuda Provide Insights Into Seasonal Hypoxia, Coral Reef Calcification, and Ocean Acidification. *Front. Mar. Sci.* 4. doi: 10.3389/fmars.2017.00036
- Bergamin, L., Marassich, A., Provenzani, P., and Romano, E. (2018). Foraminiferal Ecozones in Two Submarine Caves of the Orosei Gulf (Sardinia, Italy). *Rendiconti. Lincei. Sci. Fisiche. e. Naturali.* 29, 547–557. doi: 10.1007/s12210-018-0700-0
- Bergamin, L., Taddei Ruggiero, E., Pierfranceschi, G., Andres, B., Costantino, R., Crovato, C., et al. (2020). Benthic Foraminifera and Brachiopods From a Marine Cave in Spain: Environmental Significance. *Mediterr. Mar. Sci.* 21, 506–518. doi: 10.12681/mms.23482
- Bermúdez, P. J. (1949). “Tertiary Smaller Foraminifera of the Dominican Republic. Special Publications of the Cushman Foundation for Foraminiferal Research 25” (Sharon, Massachusetts: Cushman Laboratory for Foraminiferal Research), 1–322
- Bishop, R. E., Humphreys, W. F., Cukrov, N., Zic, V., Boxshall, G. A., Cukrov, M., et al. (2015). ‘Anchialine’ Redefined as a Subterranean Estuary in a Crevicular or Cavernous Geological Setting. *J. Crustacean. Biol.* 35, 511–514. doi: 10.1163/1937240X-00002335
- Bornemann, J. G. (1855). Die Mikroskopische Fauna Des Septarienthones Von Hermsdorf Bei Berlin. *Z. der. Deutschen. Geologischen. Gesellsch.* 7, 307–371.
- Brady, H. B. (1881). Notes on Some of the Reticularian Rhizopoda of the “Challenger” Expedition. Part III. *Q. J. Microscopic. Sci.* 21 (81), 31–71. doi: 10.1242/jcs.s2-21.81.31
- Brady, G. S., and Robertson, D. (1870). The Ostracoda and Foraminifera of Tidal Rivers. *Ann. Magaz. Natural Histor.* 6, 1–33. doi: 10.1080/00222937008696200
- Brankovits, D., Little, S. N., Tamalavage, A. E., Mejía-Ortiz, L. M., Maupin, C. R., Yáñez-Medozo, G., et al. (2021). Changes in Organic Matter Deposition can Impact Benthic Marine Meiofauna in Karst Subterranean Estuaries. *Front. Environ. Sci.* 9. doi: 10.3389/fenvs.2021.670914
- Brankovits, D., Pohlman, J. W., Niemann, H., Leigh, M. B., Leewis, M. C., Becker, K. W., et al. (2017). Methane- and Dissolved Organic Carbon-Fueled Microbial Loop Supports a Tropical Subterranean Estuary Ecosystem. *Nat. Commun.* 8, 1835. doi: 10.1038/s41467-017-01776-x
- Bretz, J. H. (1960). Bermuda: A Partially Drowned, Late Mature, Pleistocene Karst. *Geol. Soc. America Bull.* 71, 1729–1754. doi: 10.1130/0016-7606(1960)71[1729:BAPDLM]2.0.CO;2

ACKNOWLEDGMENTS

We acknowledge field and logistical support of S. R. Smith (Bermuda Museum, Aquarium, and Zoo), G. Nolan, and B. Williams. This work approved through the support of a Special Permit (2015, Permit Number 150301 to PvH) from the Department of Environmental Protection in the Bermuda Government. This research is only possible through the long-term support from the Tucker family, the Bermuda National Trust, members of the Bermuda Zoological Society, and property owners who provide access to cave entrances. Jason Richards is thanked for sharing the cave survey, which increasing the usability of these results to all future researchers.

SUPPLEMENTARY MATERIAL

The Supplementary Material for this article can be found online at: <https://www.frontiersin.org/articles/10.3389/fmars.2022.893867/full#supplementary-material>

- Carmen, K. W. (1927). *The Shallow-Water Foraminifera of Bermuda* (Cambridge: Massachusetts Institute of Technology).
- Cate, J. R. (2009). *Assessing the Impact of Groundwater Pollution From Marine Caves on Nearshore Seagrass Beds in Bermuda*, MSc, Texas A&M University.
- Chapman, F., Parr, W. J., and Collins, A. C. (1934). Tertiary Foraminifera of Victoria, Australia. The Balcombian Deposits of Port Phillip. Part Iii. *J. Linn. Soc. Lond. Zool.* 38, 553–577. doi: 10.1111/j.1096-3642.1934.tb00996.x
- Charette, M. A., and Sholkovitz, E. R. (2002). Oxidative Precipitation of Groundwater-Derived Ferrous Iron in the Subterranean Estuary of a Coastal Bay. *Geophys. Res. Lett.* 29 (10). doi: 10.1029/2001GL014512
- Chávez-Solís, M., Solís, C., Simões, N., and Mascaró, M. (2020). Distribution Patterns, Carbon Sources and Niche Partitioning in Cave Shrimps (Atyidae: Typhlatya). *Sci. Rep.* 10, 12812. doi: 10.1038/s41598-020-69562-2
- Clarke, K. R., Somerfield, P. J., and Gorley, R. N. (2008). Testing of Null Hypotheses in Exploratory Community Analyses: Similarity Profiles and Biota-Environment Linkage. *J. Exp. Mar. Biol. Ecol.* 366, 56–69. doi: 10.1016/j.jembe.2008.07.009
- Collins, S. V., Reinhardt, E. G., Werner, C. L., Le Maillot, C., Devos, F., and Rissolo, D. (2015). Late Holocene Mangrove Development and Onset of Sedimentation in the Yax Chen Cave System (Ox Bel Ha) Yucatan Mexico: Implications for Using Cave Sediments as a Sea-Level Indicator. *Palaeogeog. Palaeoclimatol. Palaeoecol.* 438, 124–134. doi: 10.1016/j.palaeo.2015.07.042
- Coutino, A., Stastna, M., McNeill-Jewer, C., and Reinhardt, E. G. (2021). Inland Tidal Oscillations Within the Yucatan Peninsula. *Geophys. Res. Lett.* 48, e2020GL092091. doi: 10.1029/2020GL092091
- Cresswell, J. N., and van Hengstum, P. J. (2021). Habitat Partitioning in the Marine Sector of Karst Subterranean Estuaries and Bermuda’s Marine Caves: Benthic Foraminiferal Evidence. *Front. Environ. Sci.* 8. doi: 10.3389/fenvs.2020.594554
- Cushman, J. A. (1922). Shallow-Water Foraminifera of the Tortugas Region. *Pub. Carnegie. Inst. Washin.* 342, 73–84.
- Cushman, J. A., and Brönnimann, P. (1948). Additional New Species of Arenaceous Foraminifera From Shallow Waters of Trinidad. *Contribu. to Lab. Foraminifer. Res.* 24, 37–42.
- Cushman, J. A., and Ponton, G. M. (1932). The Foraminifera of the Upper, Middle, and Part of the Lower Miocene of Florida. *Florida State. Geol. Surv. Bull.* 9, 147.
- Czjzek, J. (1848). Beitrag Zur Kenntniss Der Fossilen Foraminiferen Des Wiener Beckens. *Naturwissenschaft. Abhandlung.* 2, 137–150.
- D’orbigny, A. D. (1839). “Foraminifères” in *Histoire Physique, Politique Et Naturelle De L’île De Cuba*. (Paris: Arthus Bertrand) vol. 191. Ed. R. Sagra
- Ehrenberg, C. G. (1843). Verbreitung Und Einfluss Des Mikroskopischen Lebens in Sud- Und Nord-Amerika. *Physikalische Abhandlungen der Königlichen Akademie der Wissenschaften zu Berlin.* 1, 291–446.

- Fichez, R. (1991a). Benthic Oxygen Uptake and Carbon Cycling Under Aphotic and Resource-Limiting Conditions in a Submarine Cave. *Mar. Biol.* 110, 137–143. doi: 10.1007/BF01313100
- Fichez, R. (1991b). Suspended Particulate Organic Matter in a Mediterranean Submarine Cave. *Mar. Biol.* 108, 167–174. doi: 10.1007/BF01313485
- Fornós, J. J., Ginés, J., and Gràcia, F. (2009). Present-Day Sedimentary Facies in the Coastal Karst Caves of Mallorca Island (Western Mediterranean). *J. Cave. Karst. Stud.* 71, 86–99.
- Fornós, J. J., Ginés, J., Gràcia, F., Merino, A., Gómez-Pujol, L., and Bover, P. (2014). Cave Deposits and Sedimentary Processes in Cova Des Pas De Vallgornera (Mallorca, Western Mediterranean). *Int. J. Speleol.* 43, 159–174. doi: 10.5038/1827-806X.43.2.5
- Fourqurean, J. W., Manuel, S. A., Coates, K. A., Kenworthy, W. J., and Boyer, J. N. (2015). Water Quality, Isoscapes and Stoichioscapes of Seagrasses Indicate General P Limitation and Unique N Cycling in Shallow Water Benthos of Bermuda. *Biogeosciences* 12, 6235–6249. doi: 10.5194/bg-12-6235-2015
- Fourqurean, J. W., Manuel, S. A., Coates, K. A., Massey, S. C., and Kenworthy, W. J. (2019). Decadal Monitoring in Bermuda Shows a Widespread Loss of Seagrasses Attributable to Overgrazing by the Green Sea Turtle *Chelonia Mydas*. *Estuar. Coast.* 42, 1524–1540. doi: 10.1007/s12237-019-00587-1
- France, R. L. (1995). Carbon-13 Enrichment in Benthic Compared to Planktonic Algae: Food Web Implications. *Mar. Ecol. Prog. Ser.* 124, 307–312. doi: 10.3354/meps124307
- Garrison, L. E. (1959). Miocene Foraminifera From the Temblor Formation North of Coalinga, California. *J. Paleontol.* 33, 662–669.
- Gonnea, M. E., Charette, M. A., Liu, Q., Herrera-Silveira, J. A., and Morales-Ojeda, S. M. (2014). Trace Element Geochemistry of Groundwater in a Karst Subterranean Estuary (Yucatan Peninsula, Mexico). *Geochem. Cosmochim. Acta* 132, 31–49. doi: 10.1016/j.gca.2014.01.037
- Gregory, B. R. B., Reinhardt, E. G., and Gifford, J. A. (2017). The Influence of Morphology on Sinkhole Sedimentation at Little Salt Spring, Florida. *J. Coas. Res.* 33, 359–371. doi: 10.2112/JCOASTRES-D-15-00169.1
- Hart, C. W. J., and Manning, R. B. (1986). Two New Shrimps (Procarididae and Agostocarididae, New Family) From Marine Caves of the Western North Atlantic. *J. Crustacean. Biol.* 6, 408–416. doi: 10.2307/1548181
- Haynes, J. R. (1973). Cardigan Bay Recent Foraminifera (Cruises of the R. V. Antur 1962–1964). Bulletin of the British Museum of Natural History. *Zoolog. Suppl.* 4, 50–52.
- Hearty, P. J. (2002). Revision of the Late Pleistocene Stratigraphy of Bermuda. *Sedimen. Geol.* 153, 1–21. doi: 10.1016/S0037-0738(02)00261-0
- Hijma, M. P., Englehart, S. E., Tornqvist, T. E., Horton, B. P., Hu, P., and Hill, D. F. (2015). “A Protocol for a Geological Sea-Level Database,” in *Handbook of Sea-Level Research*. Eds. I. Shennan, A. J. Long and B. P. Horton (Chichester: John Wiley & Sons, Ltd), 536–553.
- Höglund, H. (1947). Foraminifera in the Gullmar Fjord and the Skagerak. *Zoolog. Bidrag. Från. Uppsala. Band.* 26, 328.
- Hunter, R. L., Webb, M. S., Iliffe, T. M., and Alvarado Bremer, J. R. (2007). Phylogeny and Historical Biogeography of the Cave-Adapted Shrimp Genus *Typhlatya* (Atyidae) in the Caribbean Sea and Western Atlantic. *J. Biogeograph.* 35, 65–75. doi: 10.1111/j.1365-2699.2007.01767.x
- Javaux, E., and Scott, D. B. (2003). Illustration of Modern Benthic Foraminifera From Bermuda and Remarks on Distributions in Other Subtropical/Tropical Areas. *Paleontol. Electronic.* 6, 29. doi: http://paleo-electronica.org/paleo/2003_1/benthic/issue1_03.htm.
- Jorissen, F. J., De Stigter, H. C., and Widmark, J. G. V. (1995). A Conceptual Model Explaining Benthic Foraminifera Microhabitats. *Mar. Micropaleontol.* 26, 3–15. doi: 10.1016/0377-8398(95)00047-X
- Juggins, S. (2015) Rioja: Analysis of Quaternary Science Data (Accessed 28 Feb 2022).
- Keyser, D. (1977). “Ecology of Zoogeography of Recent Brackish-Water Ostracods (Crustacea) From South-West Florida,” in *Aspects of the Ecology and Zoogeography of Recent and Fossil Ostracoda*. Eds. H. Löffler and D. Danielpol (The Hague: Dr. W. Junk Publishers), 207–222.
- Keyser, D., and Schöning, C. (2000). Holocene Ostracoda (Crustacea) From Bermuda. *Senckenberg. Leth.* 80, 567–591. doi: 10.1007/BF03043366
- Kitamura, A., Yamamoto, N., Kase, T., Ohashi, S., Hiramoto, M., Fukusawa, H., et al. (2007). Potential of Submarine-Cave Sediments and Oxygen Isotope Composition of Cavernicolous Micro-Bivalve as a Late Holocene Paleoenvironmental Record. *Global Planet. Change* 55, 301–316. doi: 10.1016/j.gloplacha.2006.09.002
- Kovacs, S. E., Reinhardt, E. G., Chatters, J. C., Rissolo, D., Schwarcz, H. P., Collins, S. V., et al. (2017). Calcite Raft Geochemistry as a Hydrological Proxy for Holocene Aquifer Conditions in Hoyo Negro and Ich Balam (Sac Actun Cave System), Quintana Roo, Mexico. *Quater. Sci. Rev.* 175, 97–111. doi: 10.1016/j.quascirev.2017.09.006
- Kovacs, S. E., Reinhardt, E. G., Werner, C., Kim, S.-T., Devos, F., and Le Maillot, C. (2018). Seasonal Trends in Calcite-Raft Precipitation From Cenotes Rainbow, Feno and Monkey Dust, Quintana Roo, Mexico: Implications for Paleoenvironmental Studies. *Palaeogeog. Palaeoclimatol. Palaeoecol. Press.* 497 (1), 157–167. doi: 10.1016/j.palaeo.2018.02.014
- Lamb, A. L., Wilson, G. P., and Leng, M. J. (2006). A Review of Coastal Paleoclimate and Relative Sea-Level Reconstructions Using $\delta^{13}C$ and C/N Ratios in Organic Material. *Earth Sci. Rev.* 75, 29–57. doi: 10.1016/j.earscirev.2005.10.003
- Land, L. S., Mackenzie, F. T., and Gould, S. J. (1967). The Pleistocene History of Bermuda. *GSA. Bull.* 78, 993–1006. doi: 10.1130/0016-7606(1967)78[993:PHOB]2.0.CO;2
- Legendre, P., and Legendre, L. (1998). *Numerical Ecology* (Amsterdam: Elsevier).
- Lisiecki, L. E., and Raymo, M. E. (2005). A Pliocene-Pleistocene Stack of 57 Globally Distributed Benthic $\delta^{18}O$ Records. *Paleoceanography* 20, 1–17. doi: 10.1029/2004PA001071
- Little, S. N., and van Hengstum, P. J. (2019). Intertidal and Subtidal Benthic Foraminifera in Flooded Caves: Implications for Reconstructing Coastal Karst Aquifers and Cave Paleoenvironments. *Mar. Micropaleontol.* 149, 19–34. doi: 10.1016/j.marmicro.2019.03.005
- Loeblich, A. R. Jr, and Tappan, H. (1987). *Foraminiferal Genera and Their Classification* (New York: Van Nostrand Reinhold Company).
- Love, R., Milne, G. A., Tarasov, L., Englehart, S., Hijma, M., Latychev, K., et al. (2016). The Contribution of Glacial Isostatic Adjustment to Projections of Sea Level Change Along the East and Gulf Coasts of North America. *Earth. Future* 4, 440–464. doi: 10.1002/2016EF000363
- Maddocks, R. F., and Iliffe, T. M. (1986). Podocopid Ostracoda of Bermudian Caves. *Stylogia* 2 (1/2), 26–76.
- Mejía-Ortiz, L. M., Yáñez, G., and López-Mejía, M. (2007). Echinoderms in an Anchialine Cave in Mexico. *Mar. Ecol.* 28, 31–34. doi: 10.1111/j.1439-0485.2007.00174.x
- Moore, W. S. (1999). The Subterranean Estuary: A Reaction Zone of Ground Water and Sea Water. *Mar. Chem.* 65, 111–125. doi: 10.1016/S0304-4203(99)00014-6
- Morris, B., Barnes, J., Brown, F., and Markham, J. (1977). *The Bermuda Marine Environment: a Report of the Bermuda Inshore Waters Investigations 1976-1977*. Bermuda Biological Station Special Publication 15, (St. Georges: Bermuda), 1-15.
- Muhs, D. R., Budahn, J. R., Prospero, J. M., Skipp, G., and Herwitz, S. R. (2012). Soil Genesis on the Island of Bermuda in the Quaternary: The Importance of African Dust Transport and Deposition. *J. Geophys. Res.* 117, F03025. doi: 10.1029/2012JF002366
- Murray, J. (2006). *Ecology and Applications of Benthic Foraminifera* (London: Cambridge University Press).
- Myroie, J. E., Carew, J. L., and Vacher, H. L. (1995). “Karst Development in the Bahamas and Bermuda” in *Terrestrial and Shallow Marine Geology of the Bahamas and Bermuda*. Eds. H. A. Curran and B. White (Boulder: Geologic Society of America Special Paper 300), 251–267.
- Natland, M. L. (1938). New Species of Foraminifera From Off the West Coast of North America and From the Later Tertiary of the Los Angeles Basin. *Tech. Ser. Bull. Scrip. Inst. Oceanog.* 4, 137–152.
- Neumann, A. C. (1965). Processes of Recent Carbonate Sedimentation in Harrington Sound, Bermuda. *Bull. Mar. Sci.* 15, 987–1035.
- Oksanen, J., Blanchet, F. G., Kindt, R., Legendre, P., Minchin, P. R., O'hara, R. B., et al. (2013). Vegan: Community Ecology Package. *R Package Ver.* 3.
- Palmer, A. N., Palmer, M. V., and Queen, J. M. (1977). “Geology and Origin of the Caves of Bermuda” in Ed.T.D. Ford *Proceedings Seventh International Speleological Congress*. (Sheffield: British Cave Research Association), 336–338.
- Patterson, R. T., and Fishbein, E. (1989). Re-Examination of the Statistical Methods Used to Determine the Number of Point Counts Needed for Micropaleontological Quantitative Research. *J. Paleontol.* 63, 245–248. doi: 10.1017/S0022336000019272

- Pawlowski, J. (1991). Distribution and Taxonomy of Some Benthic Tiny Foraminifers From the Bermuda Rise. *Micropaleontology* 37, 163–172. doi: 10.2307/1485556
- Peltier, W. R. (2004). Global Glacial Isostasy and the Surface of the Ice-Age Earth: The ICE-5G Model and Grace. *Annu. Rev. Earth Planet. Sci.* 32, 111–149. doi: 10.1146/annurev.earth.32.082503.144359
- Phleger, F. B., Parker, F. L., and Peirson, J. F. (1953). North Atlantic Foraminifera. *Reports of the Swedish Deep-Sea Expedition* 7(1), 1–122.
- Pirsson, L. V. (1914). Geology of Bermuda Island: The Igneous Platform. *Am. J. Sci.* 38, 189–206. doi: 10.2475/ajs.s4-38.225.189
- Pirsson, L. V., and Vaughn, T. W. (1917). A Deep Boring in Bermuda Island. *Am. J. Sci. Ser. 4* 36, 70–71. doi: 10.2475/ajs.s4-36.211.70
- Proctor, C. J., and Smart, P. L. (1991). A Dated Sediment Record of Pleistocene Transgressions on Perry Head, Southwest England. *J. Quater. Sci.* 6, 233–244. doi: 10.1002/jqs.3390060306
- Radolović, M., Bakran-Petricioli, T., Petricioli, D., Surić, M., and Perica, D. (2015). Biological Response to Geochemical and Hydrological Processes in a Shallow Submarine Cave. *Mediterr. Mar. Sci.* 16, 305–324. doi: 10.12681/mms.1146
- Reuss, A. E. (1850). Neue Foraminiferen Aus Den Schichten Des Österreichischen Tertiärbeckens. *Denkschrift. der. Kaiserlich. Akad. der. Wissenschaft.* 1, 365–390.
- Rhumbler, L. (1906). Die Foraminiferen Von Laysan Und Den Chatham-Inseln. *Zoolog. Jahrbücher.* 24, 21–80.
- Richards, D. A., Smart, P. L., and Edwards, R. L. (1994). Maximum Sea Levels for the Last Glacial Period From U-series Ages of Submerged Speleothems. *Nature* 367, 357–360. doi: 10.1038/367357a0
- Riedl, R., and Ozretić, B. (1969). Hydrobiology of Marginal Caves. Part 1: General Problems and Introduction. *Int. Rev. Des. Gesam. Hydrobiolog. und Hydrograph.* 54, 661–683. doi: 10.1002/iroh.19690540503
- Roe, H. M., and Patterson, R. T. (2006). Distribution of Thecamoebians (Testate Amoebae) in Small Lakes and Ponds, Barbados, West Indies. *J. Foraminifer. Res.* 36, 116–134. doi: 10.2113/36.2.116
- Rohling, E. J., Foster, G. L., Grant, K. M., Marina, G., Roberts, A. P., Tamsiea, M. E., et al. (2014). Sea-Level and Deep-Sea-Temperature Variability Over the Past 5.3 Million Years. *Nature* 508, 477–482. doi: 10.1038/nature13230
- Romano, E., Bergamin, L., Di Bella, L., Frezza, V., Marassich, A., Pierfranceschi, G., et al. (2020). Benthic Foraminifera as Proxies of Marine Influence in the Orseoi Marine Caves (Sardinia, Italy). *Aquat. Conserv.: Mar. Freshw. Ecosys.* 30, 701–716. doi: 10.1002/aqc.3288
- Romano, E., Bergamin, L., Pierfranceschi, G., Provenzani, C., and Marassich, A. (2018). The Distribution of Benthic Foraminifera in Bel Torrente Submarine Cave (Sardinia, Italy) and Their Environmental Significance. *Mar. Environ. Res.* 133, 114–127. doi: 10.1016/j.marenvres.2017.12.014
- Roy, M., Martin, J. B., Cherrier, J., Cable, J. E., and Smith, C. G. (2010). Influence of Sea Level Rise on Iron Diagenesis in an East Florida Subterranean Estuary. *Geochim. Cosmochim. Acta.* 74, 5560–5573.
- Sanz, S., and Platvoet, D. (1995). New Perspectives on the Evolution of the Genus *Typhlatya* (Crustacea, Decapoda): First Record of a Cavernicolous Attyid in the Iberian Peninsula, *Typhlatya Miravetensis* N.Sp. *Contribut. to Zoolog.* 65, 79–99. doi: 10.1163/26660644-06502002
- Sayes, R. W. (1931). Bermuda During the Ice Ages. *Proc. Am. Acad. Art. Sci.* 66, 381–468. doi: 10.2307/20026356
- Scott, D. B. (1976). Brackish-Water Foraminifera From Southern California and Description of *Polysaccamina Ipohalina* N. Gen., N. Sp. *J. Foraminifer. Res.* 6, 312–321. doi: 10.2113/gsjfr.6.4.312
- Scott, D. B., and Hermelin, J. O. R. (1993). A Device for Precision Splitting of Micropaleontological Samples in a Liquid Suspension. *J. Paleontol.* 67, 151–154. doi: 10.1017/S0022336000021302
- Scott, D. B., Mediol, F. S., and Schafer, C. T. (2001). *Monitoring in Coastal Environments Using Foraminifera and Thecamoebians Indicators* (Cambridge: Cambridge University Press).
- Scott, D. B., and Vilks, G. (1991). Benthic Foraminifera in the Surface Sediments of the Deep-Sea Arctic Ocean. *J. Foraminifer. Res.* 21, 20–38. doi: 10.2113/gsjfr.21.1.20
- Shinn, E. A., Reich, C. D., Locker, S. D., and Hine, A. C. (1996). A Giant Sediment Trap in the Florida Keys. *J. Coas. Res.* 12, 953–959.
- Spiteri, C., Regnier, P., Slomp, C. P., and Charette, M. A. (2006). pH-Dependent Iron Oxide Precipitation in a Subterranean Estuary. *J. Geochem. Explor.* 88, 399–403.
- Stock, J. H., Iliffe, T. M., and Williams, D. (1986). The Concept "Anchialine" Reconsidered. *Stylogia* 2, 90–92.
- Stoffer, J. L. (2013). *A Hydrological Model of Harrington Sound, Bermuda and its Surrounding Cave Systems* (M. Sc., Texas A&M University).
- Tamalavage, A. E., van Hengstum, P. J., Louchouart, P., Kaiser, K., Donnelly, J. P., Albury, N. A., et al. (2018). Organic Matter Sources and Lateral Sedimentation in a Bahamian Karst Basin (Sinkhole) Over the Late Holocene: Influence of Local Vegetation and Climate. *Palaeogeog. Palaeoclimatol. Palaeoecol.* 506, 70–83. doi: 10.1016/j.palaeo.2018.06.014
- Vacher, H. L., and Rowe, M. P. (1997). "Geology and Hydrogeology of Bermuda," in *Geology and Hydrogeology of Carbonate Islands*. Eds. H. L. Vacher and T. M. Quinn (Amsterdam: Elsevier), 35–90.
- van Hengstum, P. J., Cresswell, J. N., Milne, G. A., and Iliffe, T. M. (2019). Development of Anchialine Cave Habitats and Karst Subterranean Estuaries Since the Last Ice Age. *Sci. Rep.* 9, 11907. doi: 10.1038/s41598-019-48058-8
- van Hengstum, P. J., Reinhardt, E. G., Beddows, P. A., and Gabriel, J. J. (2010). Investigating Linkages Between Holocene Paleoclimate and Paleohydrogeology Preserved in a Yucatan Underwater Cave. *Quater. Sci. Rev.* 29, 2788–2798. doi: 10.1016/j.quascirev.2010.06.034
- van Hengstum, P. J., Reinhardt, E. G., Beddows, P. A., Huang, R. J., and Gabriel, J. J. (2008). Thecamoebians (Testate Amoebae) and Foraminifera From Three Anchialine Cenotes in Mexico: Low Salinity (1.5 - 4.5 Psu) Faunal Transitions. *J. Foraminifer. Res.* 38, 305–317. doi: 10.2113/gsjfr.38.4.305
- van Hengstum, P. J., Reinhardt, E. G., Beddows, P. A., Schwarcz, H. P., and Garbriel, J. J. (2009). Foraminifera and Testate Amoebae (Thecamoebians) in an Anchialine Cave: Surface Distributions From Aktun Ha (Carwash) Cave System, Mexico. *Limnol. Oceanog.* 54, 391–396. doi: 10.4319/lo.2009.54.1.0391
- van Hengstum, P. J., Richards, D. A., Onac, B. P., and Dorale, J. A. (2015). "Coastal Caves and Sinkholes." in *Handbook of Sea-level Research*. Eds. I. Shennan, A. J. Long and B. P. Horton (Chichester: John Wiley and Sons).
- van Hengstum, P. J., and Scott, D. B. (2011). Ecology of Foraminifera and Habitat Variability in an Underwater Cave: Distinguishing Anchialine Versus Submarine Cave Environments. *J. Foraminifer. Res.* 41, 201–229. doi: 10.2113/gsjfr.41.3.201
- van Hengstum, P. J., and Scott, D. B. (2012). Sea-Level Rise and Coastal Circulation Controlled Holocene Groundwater Development and Caused a Meteoric Lens to Collapse 1600 Years Ago in Bermuda. *Mar. Micropaleontol.* 90-91, 29–43. doi: 10.1016/j.marmicro.2012.02.007
- van Hengstum, P. J., Scott, D. B., Gröcke, D. R., and Charette, M. A. (2011). Sea Level Controls Sedimentation and Environments in Coastal Caves and Sinkholes. *Mar. Geol.* 286, 35–50. doi: 10.1016/j.margeo.2011.05.004
- Vollbrecht, R. (1996). *Postglazialer Anstieg Des Meeresspiegels, Paläoklima Und Hydrographie, Aufgezeichnet in Sedimenten Der Bermuda Inshore Waters* (Universität Göttingen: PhD).
- Whitaker, D., and Christman, M. (2014) Clustsig: Significant Cluster Analysis (Accessed 28 February 2022).
- Williamson, W. C. (1858). *On the Recent Foraminifera of Great Britain* (London: Ray Society).
- Williams, D. D., and Williams, N. E. (1998). Freshwater Invertebrates From the Bermuda Islands and Their Zoogeographical Affinities. *Trop. Zool.* 11, 353–369. doi: 10.1080/03946975.1998.10539371
- Woolard, G. P., and Ewing, M. (1939). Structural Geology of the Bermuda Islands. *Nature* 143, 898. doi: 10.1038/143898a0

Conflict of Interest: The authors declare that the research was conducted in the absence of any commercial or financial relationships that could be construed as a potential conflict of interest.

Publisher's Note: All claims expressed in this article are solely those of the authors and do not necessarily represent those of their affiliated organizations, or those of the publisher, the editors and the reviewers. Any product that may be evaluated in this article, or claim that may be made by its manufacturer, is not guaranteed or endorsed by the publisher.

Copyright © 2022 Cresswell and van Hengstum. This is an open-access article distributed under the terms of the Creative Commons Attribution License (CC BY). The use, distribution or reproduction in other forums is permitted, provided the original author(s) and the copyright owner(s) are credited and that the original publication in this journal is cited, in accordance with accepted academic practice. No use, distribution or reproduction is permitted which does not comply with these terms.